MATERIAL IDENTIFICATION AND CHARACTERIZATION OF THEIR PROPERTIES FOR SCALED BASE ISOLATION EXPERIMENTS

By

Yusuf GUZEL

Supervisor: Dr. Sean WILKINSON

Senior Lecturer in Structural Engineering

"Submitted in partial fulfilment of the requirements for the degree of Master of Science in Structural Engineering in the Faculty of Science Agriculture and Engineering: School of Civil Engineering and Geosciences, Newcastle University"

Address: Newcastle upon Tyne, Tyne and Wear NE1 7RU United Kingdom

Submission Date: 15/8/2014

DECLARATION

"I hereby certify that this work is my own, except where otherwise acknowledged, and that it has not been submitted previously for a degree at this or other university."

Yusuf GUZEL

ACKNOWLEDGEMENT

I am proudly willing to pay my full respect to Allah, allowing me to study in Newcastle University, one of the top ranked UK Universities. Secondly, I wish Turkish Government peace and wealth during the lifetime of the planet, which fully funds my master education fees.

I am also proud of being a master research student of Sean Wilkinson whose contributions to my project is indisputably appreciable. He helps me to broaden my horizon about earthquake engineering which is the field where I want to go through in my academic future life.

Moreover, I would like to express my gratitude to my wife, Fidan Guzel whose encouragement enables me to complete my project successfully, and my extended family whose presences in my life make me feel strong.

Lastly, I am grateful to thanks to the lecturers in the field of structural and geotechnical engineering because of their contributions to my academic life through their modules.

ABSTRACT

Base isolation devices are the best means of protecting structural and non-structural elements from damaged as well as guaranteeing life safety during and after a seismic action. One of the ways to assess the response of the base isolated structure under the dynamic earthquake load is to conduct physical testing, namely shaking table test. Representation of the real base isolated structure on a shaking table usually requires using a scaled model. The material used for the elements (columns, beams, slabs and bearings) of the model play a vital role in ensuring the test results that can be transposed to the real structure. In this project, it is aimed to identify materials for scaled base isolation (bearing) experiments, which has not been enlarged beyond the materials used in full-scale bearing. In order to do that, four-story base isolated RC medical structure has been selected as a real structure and the bearing type of the structure is HDRB with 0.75 m diameter, 0.55 m height and 36.75 shape factor. Only the first story has been considered for scaling because applying scaling laws to whole structure is complicated task that cannot be manageable in this allocated time. First story of the considered structure has been scaled by taking into account the capacity of the shaking table with applying length scale factor of 1/10 and Young's modulus scale factor of 6,67. Seven earthquake records have been selected in accordance with the code requirement (EC8) and for the model the average earthquake motion has been compressed with scale factor of 0.13 for the purpose of making the motion suitable with the period of the model. Firstly, the real structure and the model one are analysed in GSA as a fixed base and depending on their displacement ratio, which is 41, the required displacement from the scaled base isolation is computed as 0.018 m in relation to the displacement of the base isolated prototype, which is essential to assign dimensions of scaled base isolation based on materials' properties. Two types of material are used (HDRB and rubber) and 5 and 6 samples have been obtained in different sizes, respectively. It is concluded

that the aspect ratios of the provided samples are not practical in comparison with real application values for a pad bearing. Nevertheless, it can be said that the stability, critical load capacity and rocking motion of the samples should be taken into consideration at 0.018 mm displacement in real scaled base isolation experiment (shaking table test) to check their validity in full sense.

Key words: base isolation system, lead rubber bearing, HDRB, scaling laws, shaking table, shifting of ground motion, rubber.

Table of Contents

List of Figures

List of Tables

Chapter 1

1.1 Introduction

Over the recent decades, the implementation of the base isolation system to the structure has been a paramount way in regard to saving human's lives and mitigating structural and non-structural damages. As highlighted by Oh et al. (2013), the functions of the base isolation system are that the system itself has enough stiffness to transfer the load of superstructure to the foundation and capable of deflecting relatively large in the horizontal direction under the seismic load. Fundamentally, base isolation systems provide low energy input motion to the superstructure. In doing so, the structures can be kept in an elastic region under the seismic load, while the isolators deflect in huge amount (as can be seen in Figure 1.1)(Oh et al., 2013).

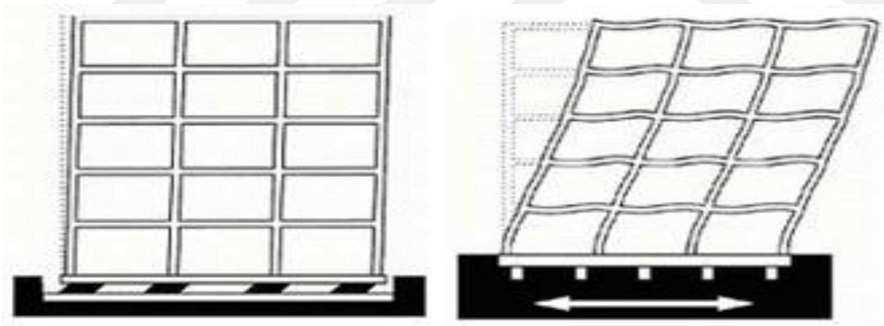

Figure 1.1 base-isolated (a) and fixed-base (b) building under lateral force (Boyer, 2013)

One of the prevailing type of the isolators is high damping lead rubber bearing which, from the point of Arya (1994), to almost full extent fulfils three main requirements: (1) carry the load of superstructure to the foundation safely, (2) allow enough lateral deflections and (3) absorb as much energy as possible under the lateral load. The reason for the effective performance of the bearing is that it dissipates energy with regular hysteresis loop produced by lead at the core under the cyclic load (hysteretic loop can be seen in Figure 1.2).

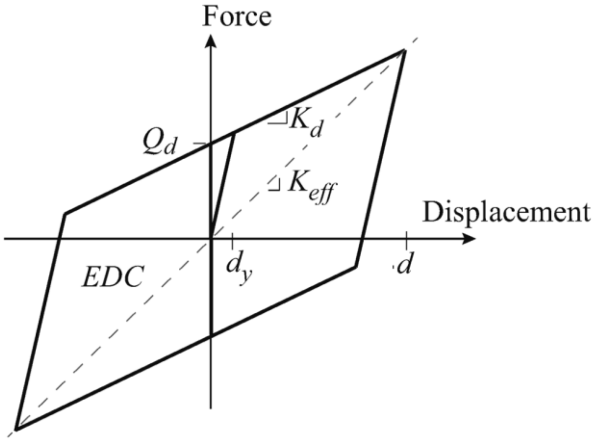

Figure 1.2 hysteresis behaviour of the lead rubber bearing ((Warn and Ryan, 2012)

With the event of Christchurch earthquake, it has been recognized that base isolation systems performed unforeseen large deformations that caused huge damages to the super-structures, which needs unreasonable repair costs of the superstructures, while human lost has been eliminated considerably. To control large displacements of the base isolation system, it has been proposed by Kelly (1999) that additional energy dissipation mechanism as of viscous damper, steel hysteretic damper, steel cantilever damper, torsional steel damper can be implemented with them.

The main vital function of the damper systems is that they generate opposite force to the oscillating force of the superstructure and they balance energy-absorbing mechanism and stiffness of the system. There are three types of damper system; passive, semi-active and active damping system. Passive damper system differs from the other two types in a way that passive ones do not need external energy power to work while the others need external energy to perform under the seismic load (Luca et al., 2005).

On the contrary, as Kelly (1999) highlights in his research that damper systems increase the stiffness of the system and that can cause the base isolation system to not behave as intended in its design. On account of that, life safety cannot be a major problem however increased floor accelerations can lead to damage of unexpected equipment. In addition to that, supplementary damper systems designed to dissipate more energy rise the inter-storey drifts, while large displacements are reduced significantly (Kelly, 1999). (Storey drift is defined by Sindel et al. (1996) as the division of the displacement value that is the difference between two adjacent floors to the height of the floor).

Figure 1.3 example of the inter-storey drift of the building (anglicantaonga, 2011)

When the base isolation systems are structured, it can be appreciated to conduct experimental tests with the view to observe elastic and inelastic behaviour of the structure. This is because simplification methods, which were commonly used until recent decades, cannot be appropriate to present complex, multi-degree of freedom system behaviour under the dynamic load (Chung et.al, 1999). Because of that matter, it is inevitable to do experimental tests to design base isolation systems of the superstructures. The most popular experimental testing methodologies are generally classified as effective force test, pseudo dynamic test, and quasistatic test, shaking table test, real time hybrid test and computational types (Jeyasehar et al., 2009). It has been claimed by Chung et al. (1999) that one of the best choices for physical testing to monitor real behaviour of the structural system is shaking table test while available shaking table has some limitations because of its displacement, maximum load, dimensions, mass and frequency capacity.

One of the most vital step for shaking table testing is to apply similitude requirements to attain a model meeting the capacity limitations of the table that represents the behaviour of a real structure in a small scale. While the elements of the real structure are scaled, base isolators should also be modelled in same sense. However, it can be possible that the materials of the real base isolators will not be the same with the materials that are liable to be used for the shaking table test.

In this project, the properties of the materials that can be potentially possible to utilize in the scaled base isolation have been characterised and the materials that have those properties have been specified by doing numerical analyses.

1.2 Aim

The aim of the project is to identify, numerically, materials that are suitable for scaled shaking table test and characterizations of their properties.

1.3 Objectives

1. Reviewing the literature of development of base isolation systems and their current implementation types.
2. Selecting a real structure that has a type of base isolation system
3. Selection of real earthquake ground motions
4. Scaling the selected structure and shifting the ground motion from objective 3
5. Modelling of the real structure and the model (scaled one) in GSA as a fixed base structure and subsequently computing displacement ratio
6. Rubber bearings modelling for the real structure and attaining displacement value that can be performed by scaled isolator
7. Quantifying the properties of the scaled isolator
8. Identifying materials which have obtained properties (in objective 7) at prescribed dimensional sizes.

1.4 The scope of the project

As mentioned in above parts, the aim of the research is to define materials and to attain the properties of them which are suitable for base isolators of the shaking table.

First step of this project is to identify base isolated building and scale its properties in accordance with scaling laws and similitude requirements. By changing the properties of the building, it is also needed to consider the change in the selected earthquake parameters of it (parameters can be period, frequency, amplitude and so on) (selections of the recorded earthquake ground motion have been done via “European strong-motion data”, available in Rexel). These changes lead to shift of the earthquake ground motion parameters because it is necessary to make every single value of real ones suitable for shaking table experiment in order to observe real behaviour of the building.

Subsequently, the materials that can potentially exhibit behaviours in a manner in which representation of the real building can be achieved in shaking table test experiments are determined (current mostly used materials are rubber, lead + rubber, Teflon).

While Arya (1994) clearly explains that lead-rubber bearing will be the best choice of base isolation system and testing that type of bearing will be more reasonable, this research will examine high damping rubber bearing in a computer software which is a type of laminated rubber bearing. The main advantages of the laminated rubber bearings to the structure can be listed as (Patil and Reddy, 2012):

- Reaction of the structure to the earthquake is reduced by 1/2-1/8
- They save their properties during cyclic load
- There is no permanent deflection

- Adequate vertical stiffness to carry the superstructure loads during dynamic and static loadings
- Consolidations in the foundation level does not make a problem for them because of their adjustability functions
- Heat stress in the superstructure is reduced by the horizontal movements of the laminated rubber bearings.

However, this project has only considered one-storey of the real structure due to the fact that applying scaling laws and similitude requirements is difficult task to do for the whole structure. Also the aim of the project does not necessitate to scale the structure wholly. Moreover, the periods of the bearings are not considered in modelling of the structure because it is needed more comprehensive and detailed research in consideration of that.

Furthermore, there has not been any physical experiments conducted in this project to compare those results with experimental ones because of the allocated time.

Chapter 2

2.1 Literature Review

Base isolation systems have been implementing to the structures with satisfactory results under the severe earthquakes. As it has been highlighted in the study of Yoo and Kim (2002), the goal of the use of base isolation system is that seismic results of relative displacements and accelerations reduce, which mostly depends on how far frequency of isolation calculated by using the stiffness of the isolators is away from effective frequency range of earthquake ground acceleration motions.

Preliminary consideration should be ground condition where the base isolation system is applied. It is worth noting that base isolation application can be reliable in the good ground condition, however in other ground conditions research should be needed, as investigating record history of the location, because undesired vertical and horizontal deformations that generally occurs in soft ground can swamp the system of isolation (Tyler, 1991).

From the first implementation, which was double concave rolling ball bearing used in U.S. (Touaillon, 1870) until now, different types of base isolation systems have been structured and developed. Especially in the recent decades, the development of seismic isolation has paced exponentially. In this part, types of bearing, EC8 prescriptions, structural model types and some material types have been reviewed.

2.1.1 Bearing

Bearing is generally classified in two types: (1) elastomeric bearing and (2) sliding bearing (Warn and Ryan, 2012).

1) Elastomeric Bearings

Elastomeric bearing is formed by two thick end plates, natural or synthetic rubber and several steel shims (Naeim and Kelly, 1999) (as can be seen from below Figure 2.1). Thick plates provide connections of the bearing to superstructure and to pads. Vulcanized rubber is bonded to the steel shims under suitable heat and pressure. The aim in the use of steel shims, as explained by Naeim and Kelly (1999), is to make bearing stiff vertically and to prevent bulging of it while there is no effect of them for horizontal stiffness.

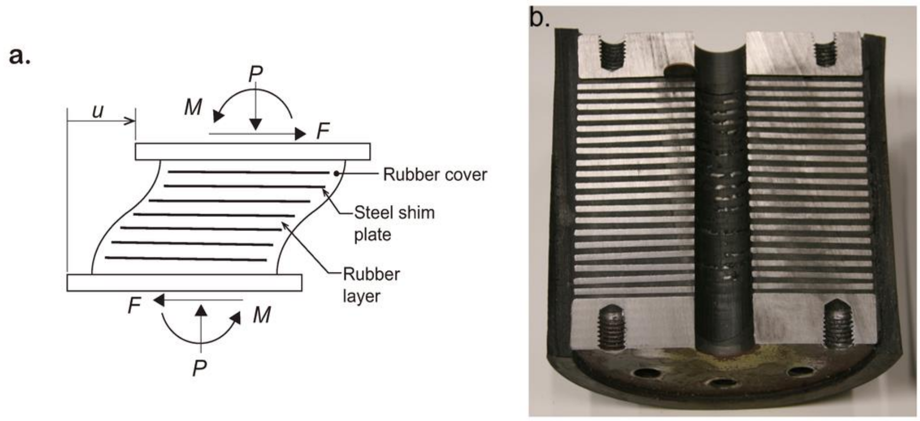

Figure 2.1 hysteretic loop of lead-rubber bearing under earthquake load (Warn and Ryan, 2012)

Low-damping natural or synthetic rubber and high-damping rubber (which is under consideration in this project) are known as the types of elastomeric bearing (Warn and Ryan, 2012). The former performs linear shear stress-strain curves with damping ratio of between 2% and 3% at shear strain of %100. The latter is obtained by adding carbon black or other fillers to the rubber which provides more damping to the bearing ranging from 10% to 20% at 100% shear strain (www.maurer-soehne.de). The advantages and disadvantages of the bearing is presented in Table 2.1 (Warn and Ryan, 2012).

Table 2.1 advantages and disadvantages of elastomeric bearing

Advantages	disadvantages
Easy to produce	Supplementary damping is needed to control large deformation
Simple to model	
Environmental factors and time does not affect mechanical behaviours	

The thickness of the elastomeric bearing increases the dominant natural period of the system by low horizontal stiffness while steel shims close to each other enable the bearing to have huge vertical stiffness (Constantinou et al., 2007).

Vertical and horizontal stiffness formulas are as follows (Kelly and Lai, 2011) (which are used in this project for stiffness calculations):

$$K_v = \frac{E_c \times A}{t_r} \tag{1}$$

$$K_h = \frac{G \times A}{t_r} \tag{2}$$

K_v= vertical stiffness of rubber bearing

K_h= horizontal stiffness of rubber bearing

E_c= instantaneous compression modulus of bearing under vertical load

G= shear modulus of rubber bearing corresponding to the shear strain

t_r= total thickness of rubber in whole bearing

E_c is under the control of the shape factor S, which is the aspect ratio of one layer of the bearing and has a given formula in equation (3).(3)(3)(3)

$$S = \frac{\text{load area}}{\text{force} - \text{free(bulge)area}} \tag{3}$$

Different shaped bearings have different shape factors and general ones are:

$S = \frac{b}{t}$ for an indefinite strip of 2b

$S = \frac{R}{2t}$ for an circular shape with radius of R

$S = \frac{a}{4t}$ for square sectional pad with a side of a length

$S = \frac{\pi \times (b^2 - a^2)}{2 \times \pi \times (a+b) \times t} = \frac{b-a}{2 \times t}$ for annular pad having inside radius a and outside radius b with thickness t.

Another form of E_c can be written as:

$$E_c = \frac{P}{A \times \epsilon_c} \quad \leftrightarrow E_c = 6 \times G \times S^2 \times \lambda \tag{4}$$

$$\lambda = \frac{(b^2 + a^2) - \dfrac{(b^2 - a^2)}{\ln(\frac{b}{a})}}{(b-a)^2} \tag{5}$$

If a/b goes 0 then $\lambda = 1$ and $E_c = 6 \times G \times S^2$ which is valid for full circular pad. Inversely, if a/b is bigger than 0.1, the value of λ closes to 2/3 which shows immense effect of small hole on E_c and, as a result, $E_c = 4 \times G \times S^2$ can be regarded.

It can be probable that rubber bearing can be critical for buckling, which is caused by low shear stiffness (Kelly and Marsico, 2013), and whether the bearing is considered as compressible or incompressible (where poisson's ratio is assumed as 0.5) can play important role in the critical loading capacity (in this project, the bearing is assumed as incompressible). It has been concluded by (Kelly, 1997) that bulk compressibility can change stiffness of bending and compression surprisingly even in the small shape factor values**.** Below formulas from the book of Kelly (1997) express the effect of bulk modulus on compression modulus and, thus, critical load pressure.

$$P_{cr} = \frac{-P_s + \sqrt{P_s^2 + 4 \times P_s \times P_E}}{2} \tag{6}$$

(P_E = Euler load for the standard column)

It is assumed that:

$$P_s \approx G \times A \tag{7}$$

$$P_E = G \times A\left(\frac{2 \times \pi^2 \times S^2 \times I}{A}\right) \tag{8}$$

Most of the bearings have a shape factor S>5 and $P_E \gg P_s$. The above equations can be written as follows:

$$P_{cr} = \sqrt{P_S \times P_E} \tag{9}$$

$$P_S = \frac{G \times A \times h}{t_r} \tag{10}$$

$$P_E = \frac{\pi^2}{h^2} \times (1/3 \times E_c \times I) \times \frac{h}{t_r} \tag{11}$$

$$P_{cr} = \frac{\sqrt{2} \times \pi \times G \times S \times A \times r}{t_r} \tag{12}$$

$$r = \sqrt{\frac{I}{A}} = \Phi/4 \tag{13}$$

(Φ is the diameter of the circular bearing)

$$p_{cr} = \frac{P_{cr}}{A} \text{ (critical pressure)} \tag{14}$$

$$S_2 = \frac{\Phi}{t_r} \text{ (second shape factor)} \tag{15}$$

$$p_{cr} = \frac{\sqrt{2}}{4} \times \pi \times G \times S \times S_2 \tag{16}$$

This critical pressure formula implies that stability of the bearing can be improved by simply increasing shape factor, layer number and reducing single layer of rubber thickness, but there is a limitation of its stability improvement because of the bulk compressibility effect(Kelly and Lai, 2011).

Different values of shape factor have been used depending on the design requirement of the rubber bearing. High shape factors can be beneficial to mitigate rocking motion and to improve stability of the bearing (Kelly, 1997). Nevertheless, it makes the vertical stiffness several hundred times bigger than horizontal stiffness and, consequently, provides vertical period to the bearing between 0.03 and 0.15 second which is undesired situation (Warn and Ryan, 2012). As a result of that, vertical accelerations increase considerably. Therefore, it can be said that the use of elastomeric bearings with high shape factors can help the structure only in horizontal direction.

In the research of Warn and Ryan (2012), it is generally design consideration of the elastomeric bearing to make the tension stress negligible. In doing so, vertical properties of the bearing can be calculated by using linear stress- strain relation. In some cases, however, it is needed to consider tension for the design of the bearing. When it is the case, instability of the bearing under tension can be possible due to the buckling.

Several studies show that critical load for buckling in compression is identical with the load that cause buckling of the bearing in tension (Kelly and Marsico, 2013). However, Kelly and Marsico (2013) explain that the presumed value of tension cannot be possible on account of cavitation of the bearing under low tension pressures. The effect of cavitation has not been understood well and, thus, more research has been needed to characterize elastomeric bearing behaviour under tension.

2) Lead-Rubber Bearing

Lead-rubber bearing is a type of elastomeric rubber bearing that only differs from the others by the lead at the centre of the bearing. The main advantages of lead rubber bearing are that (1) it has a hysteretic shear stress-shear strain relationship, which is needed for earthquake energy absorption, (2) a vertical load carrying capacity and (3) a feature of being flexible in the horizontal direction under the seismic motion (Robinson, 1982). The bearing has two important features: first one is the post-elastic stiffness (second-slope stiffness) mostly controlled by the rubber and the second one, which is associated with characteristics of the lead at the core, is the zero-displacement force-intercept (Kalpakidis and Constantinou, 2009).

The lead at the core is the key to dissipate the earthquake energy because of the fact that the lead can keep its original properties under the horizontal load, which is named as "hot working" (Robinson and Tucker, 1977). There are two ways of obtaining lead-rubber bearing: one way is to replace centre of elastomeric bearing to lead plug and the another way is before combining steel shims and rubbers together the hole can be adjusted and the lead can be machined (Robinson, 1982). Robinson (1982) has also concluded that it is reasonable to put lead plug that has a volume 1% more than the hole adjusted to ensure that it suits tightly. In doing so, it has been ascertained that when the lead-rubber bearing imposes horizontal load, the lead performs only pure shear with its whole volume.

Mechanical properties of the lead-rubber bearing can be formulated as follows (Warn and Ryan, 2012):

- $$Q_d = \sigma_L \times A_L \tag{17}$$

  Where Q_d is the zero-displacement force-intercept, σ_L is the yield strength of the lead under horizontal load and A_L is the cross sectional area of the lead plug.

- The effective stiffness of the lead-rubber bearing at the horizontal displacement d is:

  $$K_{eff} = \frac{Q_d}{d} + K_d \tag{18}$$

  Where K_d is named as second-slope stiffness and is the normal horizontal stiffness of the elastomeric bearing.

- Vertical stiffness of the lead-rubber bearing is calculated using the same formula used in the calculation of that of elastomeric bearing. The difference, however, is the effective shear modulus has been derived by considering increase of vertical stiffness because of lead at the centre.

  $$E_c = 6 \times G_{eff} \times S^2 \tag{19}$$

However, the problem in the lead-rubber bearing is the heat produced by lead at the core under the cyclic load. When the rubber bearing is subjected to horizontal cyclic load, the lead at the core imposes heating that is transferring in the vertical and radial direction to the steel shims and end plates (Kalpakidis and Constantinou, 2009). It is also explained that heat conduction of the rubber layers is ignored because rubber has a small thermal conductivity comparing to steel (Constantinou et al., 2007). On the contrary, Constantinou et al. (2007) conclude that there is no considerable heating produced in the rubber bearing under the cyclic load.

When the number of load cycles increases, the characteristic strength and the energy dissipated per cycle reduce significantly because of heat generated in the lead (Kalpakidis and Constantinou, 2009). It is evidently shown in the research of Kalpakidis and Constantinou (2009) that the energy dissipated per cycle intends to be constant after a certain number of cycle as the lead temperature reaches the constant value when the generated heat value is equal to the rate of heat lost which is done by steel shims and end plates. They summarize the behaviour of the bearing by interrupting the test in a short time and restarting cyclic loading and observing that EDC (energy dissipated per cycle) starts with almost the same level of first one. This clearly explains that, firstly, the heat increase at the core decreases the value of EDC and, secondly, lead-rubber bearing has an ability to recover its mechanical properties after a certain time from the cease of loading.

3) Sliding Bearings

Friction pendulum systems (FPS) are mainly composed of two parts: one part is concave sliding surface and the other part is an articulated slider (Al-Hussaini et al., 1994). Sliding bearings are generally made of polytetrafluoroethylene (PTFE) kind of material and for the interface, in which it is required to have a low coefficient of friction to constrain maximum resistance capacity under the horizontal forces, stainless steel is used (Warn and Ryan, 2012). There are two main advantages of the sliding isolators: (1) they have an effective performance under the range of earthquake ground motion and (2) their mechanisms itself provide enough frictional force to the force created by the acceleration of the motion (Rao and Jangid, 2001). In addition to the above advantages, the sliding bearings minimize the acceleration of the superstructure with an acceptable level of displacement, which are the main design requirements of the isolation system (Mostaghel and Khodaverdian, 1987).

As can be seen in below Figure 2.2, when the spherical concave dish moves in the horizontal direction under the seismic load, it leads to increase in the mass imposed the isolator by the superstructure (Naeim and Kelly, 1999). At the same time, Naeim and Kelly (1999) points out in their research that, the friction force produced by relative movement of spherical concave dish to the base plate over articulated slider resists the seismic load and dissipate the energy of the earthquake while spherical concave dish has an ability of restoring force (Warn and Ryan, 2012).

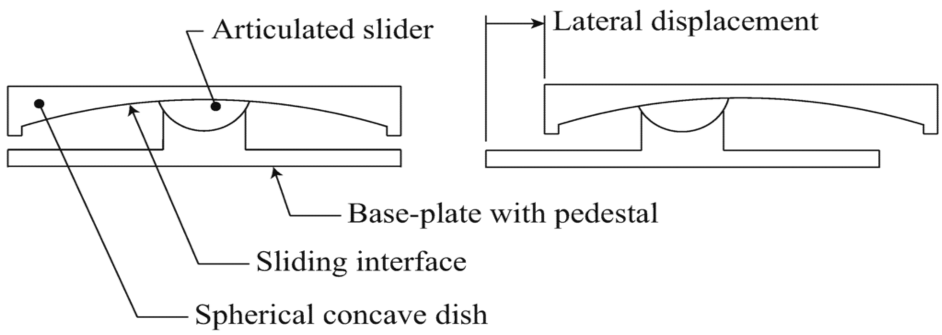

Figure 2.2 parts of single frictional pendulum bearing (Warn and Ryan, 2012)

It has been articulated by Mokha et al. (1996) that the FPS bearing is only active in the situation where horizontal force exceeds the static friction force. The static friction force known as breakaway friction force is the boundary that beyond maximum value of it where the sliding bearing is activated kinetic or sliding friction force is generated (Constantinou et al., 2007).

Lateral force is responded by both frictional force and restoring force produced by gravity load. The formula for the lateral force is as given below (Mokha et al., 1996):

$$F = \left(\frac{W}{R} \times u + \mu \times W \times \sin \dot{u}\right) \quad (20)$$

$W =$ supported weight, $R =$ radius of curvature of spherical surface,
$u =$ displacement of bearing, $\mu =$ coefficient of sliding friction,
$\dot{u} =$ velocity of bearing sliding

Based on above formula, it is obvious to say that there is a direct proportional relationship between weight of the superstructure and the seismic load. This makes the stiffness and horizontal resistance of the bearing to converge at the same point and, thus, minimize the risk of torsion because of eccentricity, whose damage is severe as it takes place (Mokha et al., 1996).

However, as Warn and Ryan (2012) demonstrate that the period of the sliding bearing does only depend on the radius of the concave dish and proven with the formula of:

$$T_d = 2 \times \pi \times \sqrt{\frac{R}{g}} \quad (21)$$

In the current decades, new type of friction pendulum bearing has been developed as double pendulum and triple pendulum bearing (Warn and Ryan, 2012). It has been expressed by Jurcau and Gillich (2009) that the double concave friction pendulum bearing, for example, has two concave interfaces and their radius and coefficients of friction can be equal or unequal. The advantages of double concave friction pendulum bearing over single one are that:

1) Two times bigger displacement capacity (Malekzadeh and Taghikhany, 2010)
2) Adaptive stiffness and damping value (this means that the stiffness and the damping properties can be in the range of calculable level at prescribed displacement) (Fenz and Constantinou, 2008).

However, single friction pendulums and multiple friction pendulums are sensitive to the tension force or uplifting, thus they are not capable of taking any tension force (Warn and Ryan, 2012). Once the tensile force is created, it will cause following damages (Roussis and Constantinou, 2006):

1. Severe damage to the bearing because of the accommodation of the superstructure load after uplifting, which will influence as crash forces
2. Contact between the superstructure and the sliding bearing can be lost
3. During the resettling of the system, columns will impose huge axial loads.

To solve tension problem in friction pendulum isolator, XY-FP isolator has been studied by Roussis and Constantinou (2006). Two orthogonal spherical stainless beam is bounded together by means of sliding system that stop the probability of uplift. Main features of the XY-FP isolator are that:

- Constraint of uplift without any effect of displacement level
- In the orthogonal directions, motions are well decoupled
- Through the each individual directions, the system has provide reliable stiffness and energy absorption mechanism.

2.1.2 Base Isolation System considered in EC8

In this part, it is willing to provide the approach of the code (EC8) to the applications and the analysis types of the base isolation system. All the information given is written in accordance with EC8.

As normal buildings have been controlled by their limit states, they should also be checked for base isolated structures. The requirement for the damage limit state is, it is needed to constrain the inter-story drift in the superstructure and the substructure, complying with the code specifications. To check ultimate limit capacity, ultimate value of the isolation devices in regard to strength and deformation should not be exceeded with considering a certain safety factor.

To enable the devices to inspect, maintain, and replace within the lifetime of the structure, it is necessary to allocate enough space between the superstructure and the substructure. Environmental effects as fire, chemical effect should also be considered.

Physical and mechanical features of the base isolator in analyses should be taken into account as the most severe values that can be obtained within the design life of the structure. Accelerations and opposing (inertia) force created by the earthquake should be assessed in relation to maximum stiffness value and the least value of friction and damping coefficients. Moreover, displacements should be related to the minimum value of stiffness, damping and friction coefficient. When the building under consideration has an importance factor of I or II, mechanical and physical properties can be averaged, keeping the variation between mean and extreme values less than %15.

Seismic actions in the two horizontal directions and the vertical direction are considered as acting at the same time. The seismic (dynamic) response of the structure can be performed in respect to inertia forces, accelerations and displacements. Effects of torsion, including accidental eccentricity, should be taken into consideration. If the following criteria are met, then, the seismic response of the structure can be described as linear equivalent:

- The effective stiffness at a displacement of $0.2d_{dc}$ (d_{dc} is design displacement) is not over two times bigger than the effective stiffness of the base isolation system.
- The effective damping ratio of the base isolation system is not greater than %30.
- Force-displacement features of the system does not change by over %10 because of the gravity loads or load rates.

Alternatively, simplified linear analysis can be used with the condition that the total eccentricity, considering also accidental eccentricity, in each horizontal direction of the plan between the mass centre of the structure and the stiffness centre of the base isolation system is not greater than %7.5 of the length of the structure in the transverse direction of the earthquake applied.

When the requirements of the equivalent linear analysis are not met, time history analysis can be applied to assess seismic response of buildings.

2.1.3 Structural Model Selection

It has been highlighted by (Sabnis et al., 1983) that "Any structural model must be designed, loaded and interpreted according to a set of similitude requirements that relate the model to the prototype structure.". In the view of this explanation, any model should be done in accordance with specific similarity rules.

The benefits and the limitations of the modelling are as follows (Dihoru et al., 2010):

Benefits

- reduction in size, simple to understand
- creating practical database/works for theoretical solutions

Limitations

- nearly impossible to fully apply similitude laws
- influence of capacity of available facilities on modelling and design
- fabrication and construction errors which affect the result.

For the structural purposes, there are 3 types of models that can be applied to the prototype, which are (Sabnis et al., 1983):

1. **The true model:** it is based on complete similarity where every arrangement between prototype and the model should suit.
2. **The adequate model:** in this model, the main characteristics of the problem should be in the control of similarity rules but second importance ones should not

be associated with the rules. Thus, this model can be named as "first-order" similarity.

3. **The distorted model:** it is not suitable for real practice because it does not totally satisfy the "first-order" similarity.

In this research, the adequate model has been selected because of its advantage of "first-order" similarity over the true and the distorted models.

This study considers the modelling as **static elastic** and the below table demonstrates scale factors for parameters that can be scaled.

Table 2.2 Similitude Requirements, Static Elastic Modelling (Dihoru et al., 2010)

	artificial mass simulation	
parameters to be scaled	**material modelled**	**prototype material**
length (L)(m)	S_L	S_L
time (t)(s)	$S_L^{1/2}$	$S_L^{1/2}$
frequency (f) (1/s)	$S_L^{-1/2}$	$S_L^{-1/2}$
velocity (v)	$S_L^{1/2}$	$S_L^{1/2}$
Gravitational acceleration (g)	1	1
acceleration (a)	1	1
mass density (ρ)	S_E/S_L	$1/S_L$
strain (ϵ)	1	1
stress (σ)	S_E	1
young's modulus (E)(GPA)	S_E	1
specific stiffness (E/ρ)	S_L	S_L
deflection (δ)	S_L	S_L
force (Q)	$S_E*S_L^2$	S_L^2
energy (EN)	$S_E*S_L^3$	S_L^3
pressure (q)	S_E	1
mass (M)(KN)	$S_E*S_L^2$	S_L^2
poisson's ratio (ν)	1	1

S_L = Length scale factor, S_E = Young's Modulus scale factor

2.1.4 Potential materials and their properties

The most commonly used materials as main components of a bearing are rubber and steel. Elastomeric bearings and sliding bearings can be examples for them, respectively and the characteristics of them have been given in the previous section. Strength and young modulus are the main identifications of the materials and the selections of them for structural uses mostly depend on the behaviour of them under the prescribed conditions. Figure 2.3 shows that different types of materials have various number of specific stiffness and strengths.

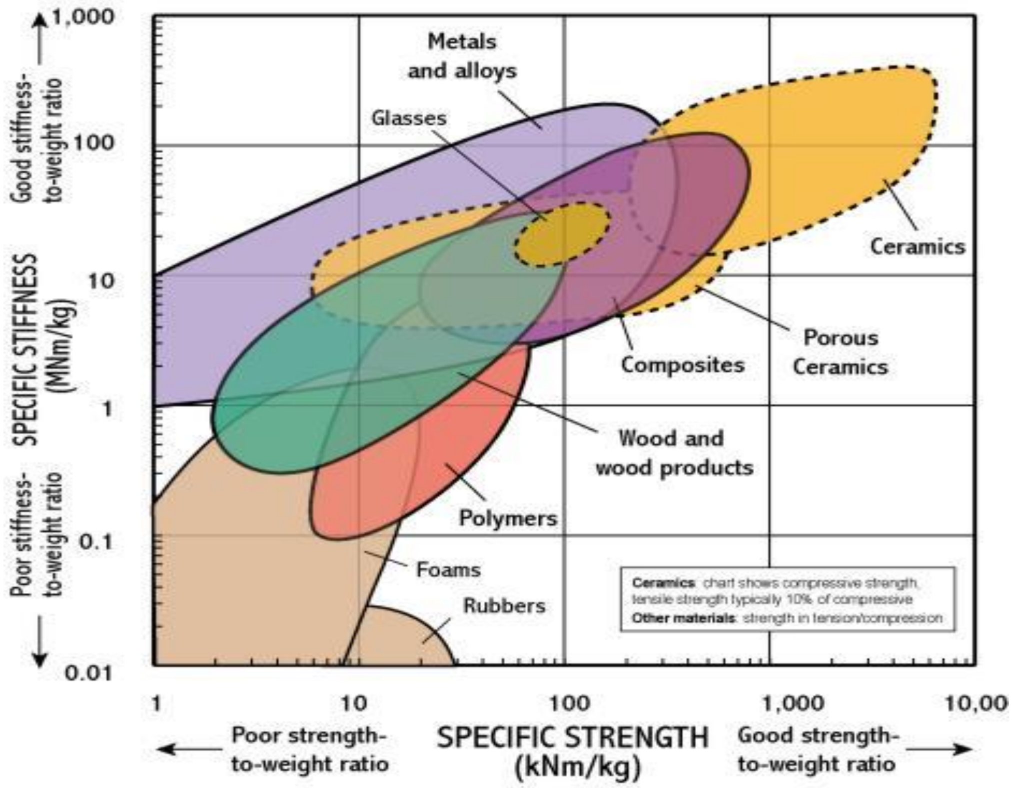

Figure 2.3 specific stiffness to specific strength for materials (from http://www-materials.eng.cam.ac.uk/mpsite/interactive_charts/spec-spec/NS6Chart.html)

In some cases, elongation of the material has as much importance as the strength and stiffness. For instance, elastomeric rubber bearings are designed to deform relatively large in the horizontal direction and it is also expected that they are stiff enough in the vertical direction to carry the superstructure loads. The given below Figure 2.4 demonstrates the strength corresponding to the elongation for different materials.

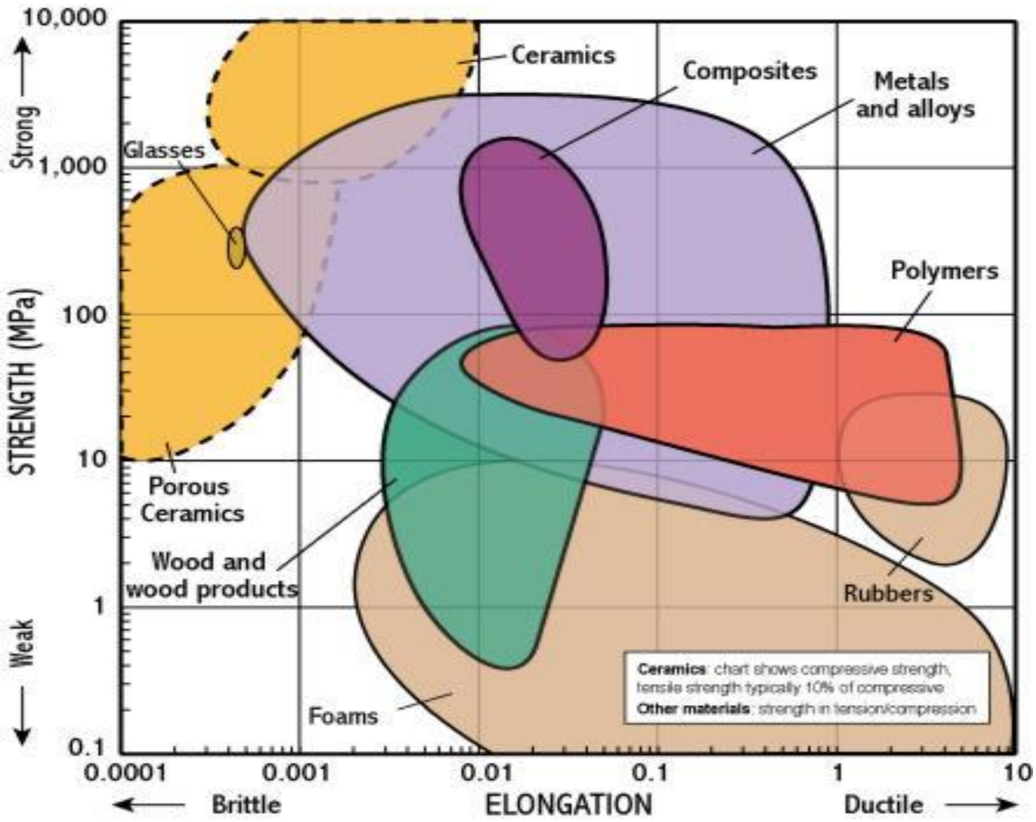

Figure 2.4 strength to elongation of the materials (from http://www-materials.eng.cam.ac.uk/mpsite/interactive_charts/spec-spec/NS6Chart.html)

Chapter 3

3.1 Methodology

In this section, it is aimed to give detail information about used real structure, instruments of the shaking table and its capacity, scale laws and recorded earthquake selection. Substantially, simplification of the model structure and GSA analyses have been introduced.

3.1.1 Details of real structure

The prototype structure selected for this study has been used in full-scale shaking table tests in Japan (Sato et al., 2011). It is four-story RC medical structure, designed to prove the benefit and drawback of the base isolation system to the medical items to the structure with respect to short and long period ground input motion by comparing with fixed-base one.

When the near-fault earthquake ground motion is considered, it is observed that, the floor accelerations have been reduced significantly by using base isolation system and, thus, the building can be occupied and operated safely. However, this advantage of the base-isolated structure over fixed-base one has not been observed explicitly as the long period ground motion is induced. The reason for that is there has not been reduction observed in floor accelerations, rather the maximum values of floor accelerations are bigger than PGA while they are still smaller than the maximum floor acceleration experienced by fixed-base structure.

General features of the building are given in the Table 3.1 and Table 3.2.

Table 3.1 the sizes of the prototype elements

	Width(m)	Depth(m)
Column	0.6	0.6
Beam	0.25	0.9
Shear wall	0.3	2.1
Base beam	1.4	1.4

Table 3.2 heights of the storeys

Storey no.	1	2	3	4
Height(m)	3.9	3.4	3.9	3.4

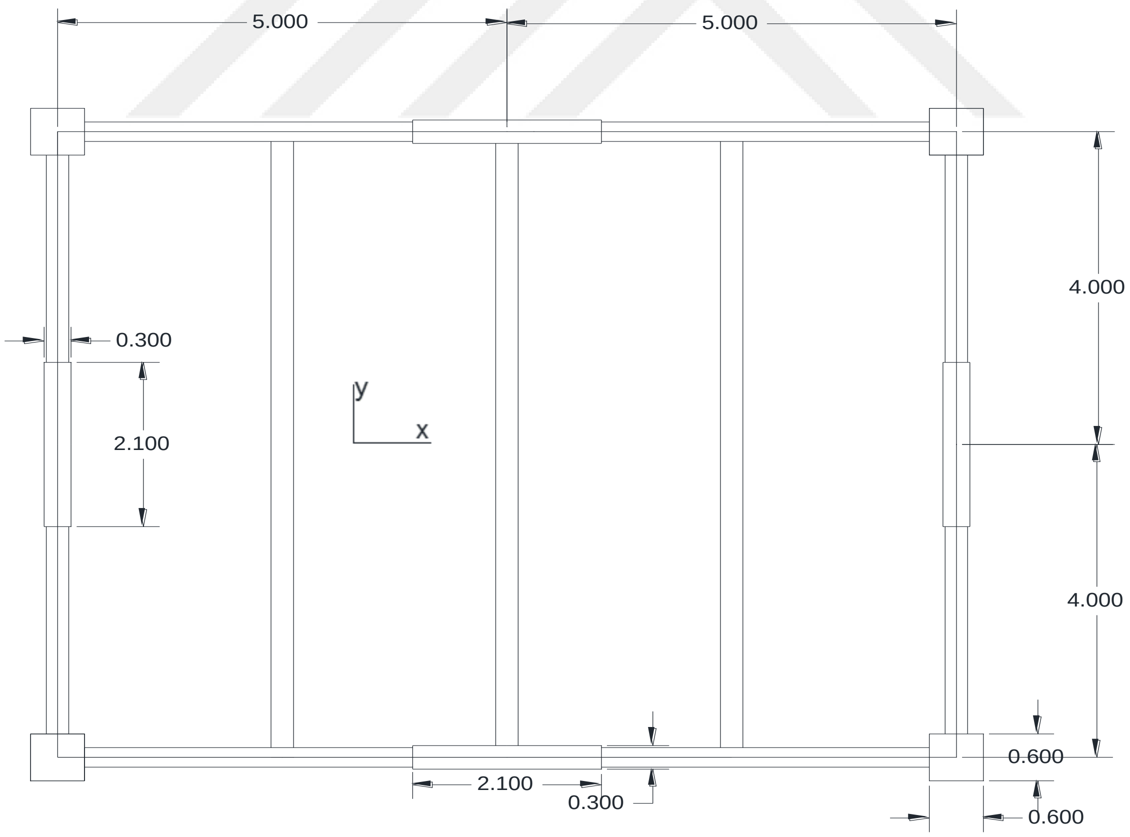

Figure 3.1 plan of the structure

In the plan of prototype, extensional parts are not drawn to simplify the model (in the real one, there are 1.4 m and 1.25 m extensions in the x and y directions of the plan, respectively). The prototype has regularity in both plan and elevation (as it is obviously demonstrated in Figure 3.1 and Figure 3.2, respectively.).

The thickness, the total height and the total mass of the prototype are 0.15 m, 16.55 m, 747 ton, respectively.

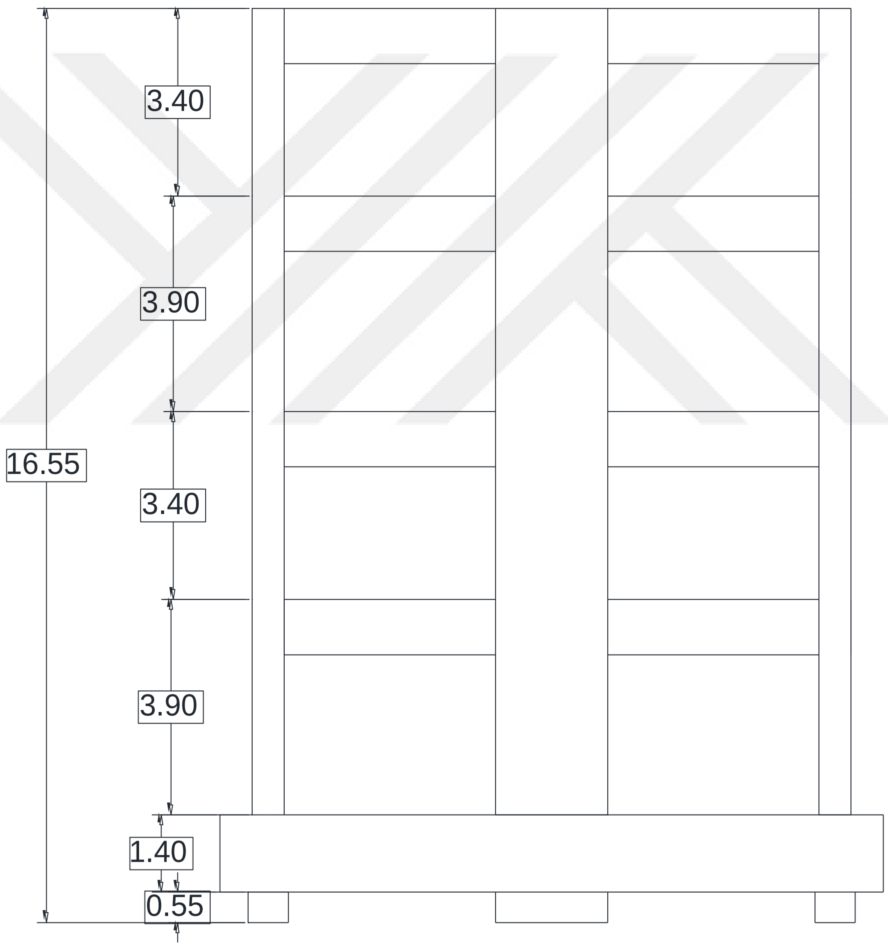

Figure 3.2 elevation of the structure (units are in metre)

3.1.2 Properties of High-damping Rubber Bearing (HDRB)

One of the bearing type used in the research of Sato et al. (2011) is high-damping rubber bearing which has properties shown in Table 3.3.

Table 3.3 properties of HDRB used in this study

Base isolator	HDRB
Diameter(mm)	750
Thickness of rubber(mm)	200
Primary shape factor (S_1)	36.75
Secondary shape factor(S_2)	3.75
Shear stiffness(KN/m)	1.37×10^3
Equivalent damping ratio	0.24
Vertical modulus(KN/m)	3.09×10^6

Shear stiffness and equivalent damping ratio is presumed for the displacement of 200 mm. The height of the bearings is not obviously given but it is assumed as 0.55 m (this assumption has been made based on the presumed depth of the base beam -given in Table 3.1 as 1.4 m- because their total height together is 1.95 m). Young's modulus and shear modulus are calculated by the formulas given in the 2.1.2 of this study (Equation (1) and Equation (2)) and the values of them are 1.4×10^6 KN/m^2 and 0.62×10^3 KN/m^2, respectively. The bearing is assumed as nearly incompressible and, thus, Poisson ratio is taken as 0.48.

It is important to note that, the periods of the rubber bearings are not considered in all GSA model analyses.

3.1.3 The properties of available shaking table

Civil engineering and Geoscience faculty at Newcastle University has a shaking table with a brand of INSRON. The capacity of the available shaking table is important to apply the scale laws/similitude requirements to the prototype structure. General properties of the table are listed as follows:

- Dimensions of the shaking table are 1100 (mm)×1100 (mm) and the model that can be suited on it has maximum dimensions of 1100 (mm)×1000 (mm)
- The displacement measurement is obtainable only in one direction
- Maximum applicable load is 20 KN
- Maximum allowed measurable displacement is 130mm in both directions of the load axis
- Likely measurement accuracy of the model on the shaking table using the laser is
  - 0.013 mm in static force
  - Between 0.013 mm and 0.1 mm in the sine wave force.
- The maximum acceleration under the applicable loading is 9.87 m/s^2.

3.1.4 Computer Software

In this research, GSA (Global Software Application) computer package programme and REXEL (v 3.5) have been used. In GSA analyses, it is aimed to (1) analyse both the prototype and the model, (2) apply the earthquake loads and (3) control the accuracy of the applied similitude laws. The analyses in GSA under the earthquake loads have been operated as **linear-**

elastic. Earthquake ground motion selection has been made by means of REXEL (Iervolino et al., 2010).

3.1.5 Prototype simplifications

Three dimensional prototype has been simplified to 2-D (Figure 3.4) and the stiffness of the structure and mass have been kept as they are to make the simplified structure representative of the structure. It is assumed that the earthquake load is applied in the x direction. New sizes of the elements of the prototype are given in Table 3.4. The lengths of the beam and column elements are kept as the same with the prototype values. In addition to this, the sizes of the base beam have not been changed due to the fact that it has big enough stiffness that can meet its design requirements.

Table 3.4 Dimensions of the elements after simplification

	Width(m)	Depth(m)
Column	0.75	0.75
Beam	0.3	1
Shear wall	0.35	2.5
Base beam	1.4	1.4

Effective width of the beam element is calculated in accordance with formulas from BRITISH STANDARD (2004a) and the sizes of the considered section is demonstrated in Figure 3.3.

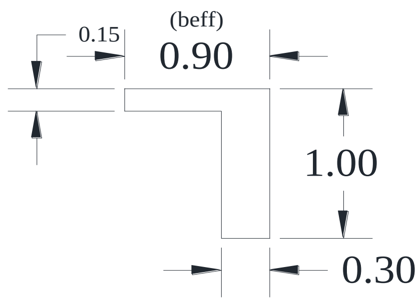

Figure 3.3 Sizes of the effective beam section (values are in metre unit)

The Young's Modulus of the reinforced concrete has been introduced to the software as 30 GPa.

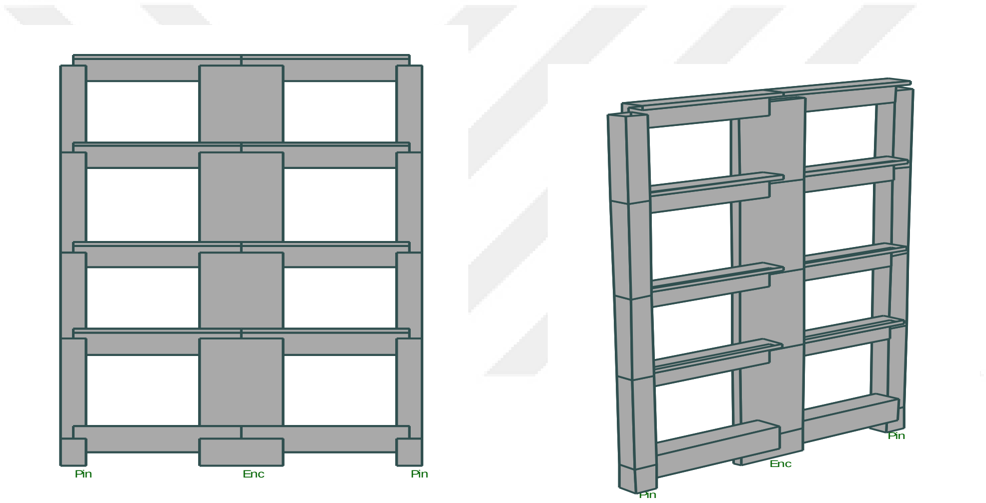

Figure 3.4 GSA 2-D model of the prototype

While the prototype has been modelled wholly in GSA as base isolated structure and fixed-base structure, whose results are expressed in the result section, this project only considers one-storey of the structure. The reasons for that are:

- Scaling whole four-storey structure is a task where it is nearly impossible to do in this projected time.
- There are limitations as mass, length, acceleration because of available shaking table.

- Lastly, the aim of project is to come up with materials that can be suitable for scaled base isolation experiment, not to scale whole structure and conduct physical testing.

The properties of the one-storey structure are directly identical to the first storey of above simplified four-storey RC structure. The only difference is that there is no shear wall modelled in one-storey structure (as can be seen in Figure 3.5). The idea in doing so is to observe pure behaviour of the rubber bearings under seismic load while it is known that shear wall elements in a structure are accepted as an earthquake resistant mechanism.

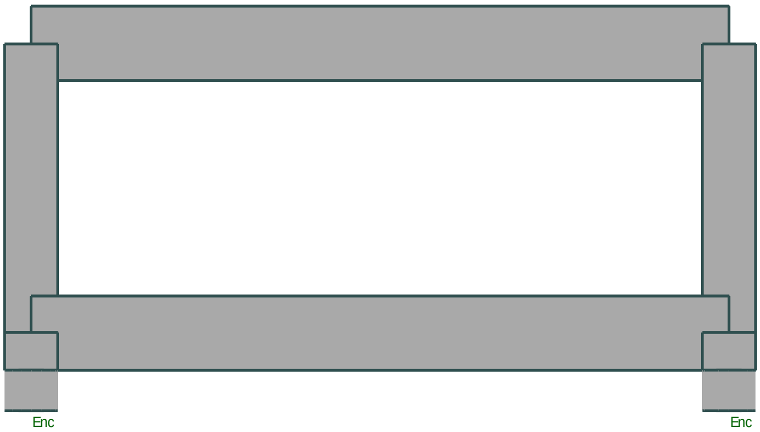

Figure 3.5 One-storey RC structure with rubber bearing (prototype)

3.1.6 Validation of the computer models

To check the validity of the computer model, one-storey of the simplified building has been modelled without base isolators and base beams and, then, the earthquake load has been applied as 1261.6 KN (which is computed by using mass (190 ton) and acceleration (6.64 m/s^2) corresponding to the period of the structure). Subsequently, the horizontal displacement of the computer model has been compared with the displacement obtained from theoretical formula of:

$$\delta = \frac{PL_c^3}{6\times E\times I_c}\left[\frac{2\times I_c\times L_s+3\times I_s\times L_c}{2\times I_c\times L_s+12\times I_s\times L_c}\right] \quad (22)$$

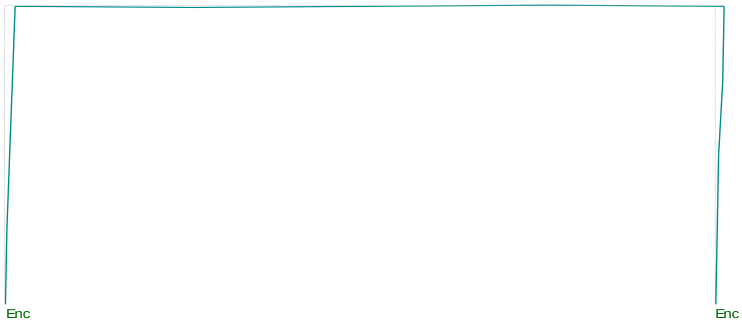

Figure 3.6 one-storey model of real structure

δ_{model}=0.015 m and

$\delta_{theoretical}$=0.0144m $\quad$ $deviation\% = \frac{|\delta_{model}-\delta_{theoretical}|}{\delta_{theoretical}} = \frac{|0.015-0.0144|}{0.0144} = 4.2\%$

There is only 4.2% deviation between two displacement values. As a result, it can be said that, the structure is modelled accurately enough and the properties are introduced properly.

3.1.7 Earthquake Ground Motion Selection

The selection of the earthquake ground motion is crucial in the analysis of the structure due to the fact that selected earthquake records should be representative of the ground motion under the considered location. There are several alternatives in the quantity of the selected earthquake but it should be at least three, in which individual analysis should be operated and the most severe resulted ground motion should be selected (BRITISH STANDARD, 2004b). In several studies like the study of Wilkinson and Sivaselvan (2008), 7 earthquake records have been accounted and the mean of them have been applied in accordance with EC8.

In this research, 7 earthquake records have been selected by using European Strong-Motion Data (Ambraseys et al., 2002). The selection criteria are as listed below:

- The location in Southern Italy with latitude of 39,314° and longitude of 16.215°
- Ground type A
- Scaled based on target spectrum of the soil type
- Magnitude(Mw) of earthquake considered between 6 and 9
- Distance from source less than 40 km.

Details of the selected earthquakes are provided in the Table 3.5.

Table 3.5 features of the selected earthquakes

EQ No.	Station ID	Earthquake Name	Date	Mw	Fault Mechanism	Epicentral Distance [km]	PGA [m/s^2]	PGV [m/s]
1	ST98	Campano Lucano	11/23/1980	6.9	normal	25	0.59	0.04
2	ST2497	South Iceland	6/17/2000	6.5	strike slip	34	0.39	0.04
3	ST539	Bingol	5/1/2003	6.3	strike slip	14	2.92	0.21
4	ST2552	South Iceland (aftershock)	6/21/2000	6.4	strike slip	24	0.58	0.07
5	ST20	Friuli	5/6/1976	6.5	thrust	23	3.50	0.21
6	ST2557	South Iceland (aftershock)	6/21/2000	6.4	strike slip	15	1.25	0.17
7	ST575	Izmit	8/17/1999	7.6	strike slip	9	1.58	0.19

3.1.8 Representativeness of selected earthquakes

The mean of selected earthquakes is compared to elastic response spectra (EC8) of the site for the purpose of ensuring that they are representative of the ground motion. To do that, firstly scale factors [SF] (as seen from Table 3.6) taken directly from REXEL are multiplied by spectral accelerations and mean of them has been figured out (Figure 3.7).

Table 3.6 scale factors for selected earthquakes

EQ No.	1	2	3	4	5	6	7
SF	5.1	7.77	1.02	5.15	0.85	2.4	1.9

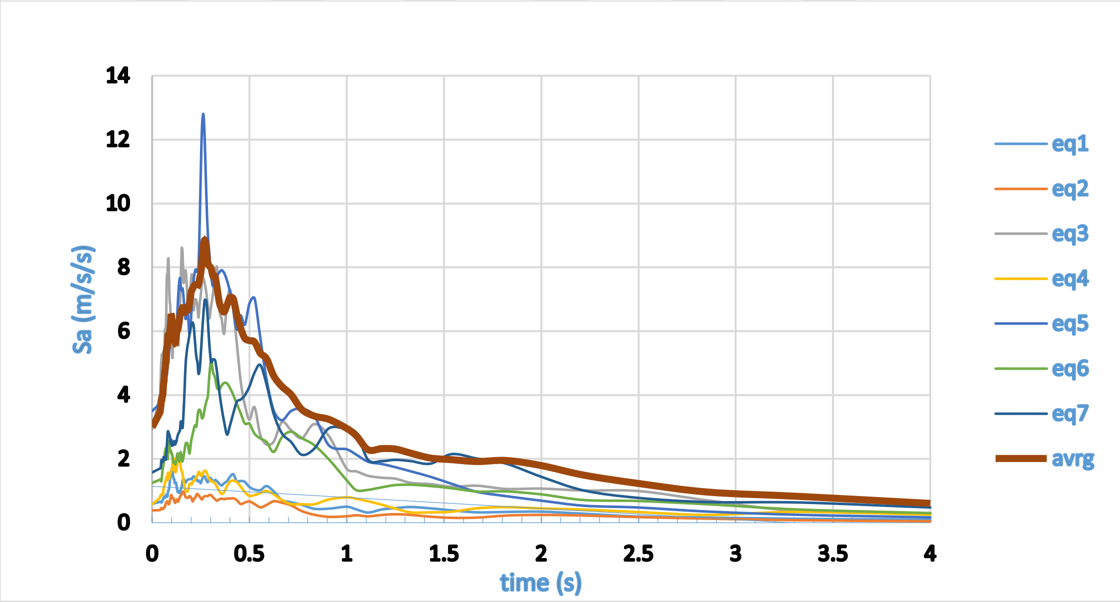

Figure 3.7 spectral accelerations of 7 selected earthquakes and their average

The mean spectral acceleration of selected earthquakes and elastic response spectra diagram can be seen in Figure 3.8.

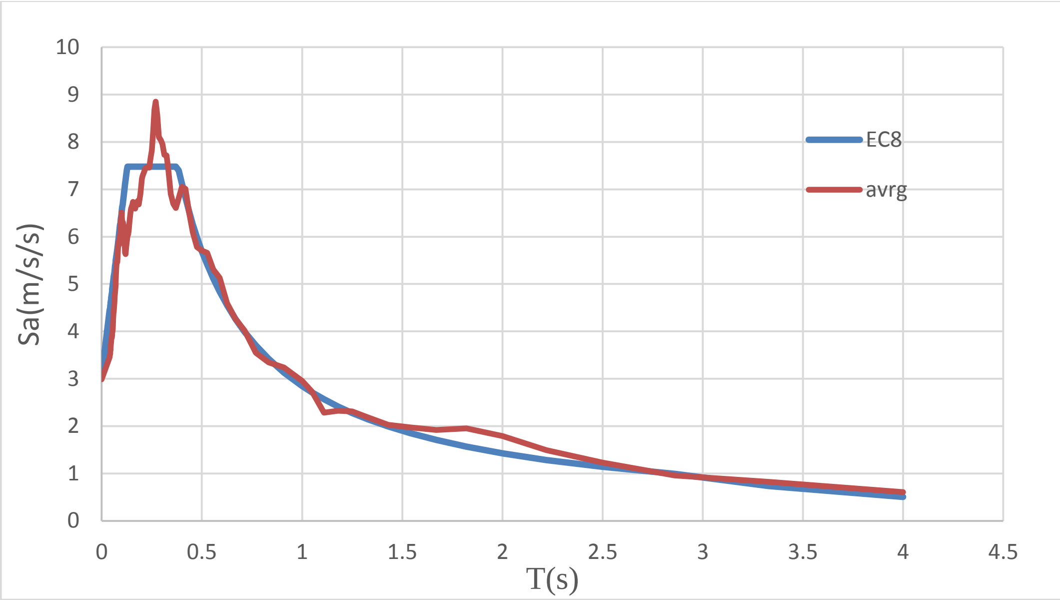

Figure 3.8 the mean spectral acceleration for seven selected earthquakes and elastic response spectra (EC8)

As it can be seen from Figure 3.8, two response spectra are almost in the same trend. This means that selected earthquakes are representative enough for an earthquake analysis of structures in that location.

3.1.9 Shifting of ground motion and spectral acceleration

In order to validate that the model is representative of the prototype, it is utmost important to change ground motion parameters, namely time step, magnitude of acceleration and elastic response spectra. The main idea to shift ground input motion is to make sure that earthquake input motion is suitable for the model of the shaking table.

The most crucial one that has to be changed is the time step of loading. The reason for that is the model of prototype has remarkably less period than the prototype (for instance in this study period for the prototype is 0.15 second and for the model it is 0.019 second) and that period is even smaller than time step of the averaged and each earthquake ground input motion. Thus, if the model is loaded with real earthquake time step, then, once the first step of loading is imposed, for instance, until second step of loading the model cycles more than one. Subsequently, the model cannot represent the prototype properly. Because of that, the ground input motion has been compressed as can be seen in Figure 3.9 and new response spectrum has been obtained as in Figure 3.10.

To apply "the adequate model", mentioned in the section 2.1.6 of this study, to the prototype to get the properties of model, it is aimed to keep S_a same for the prototype and the model. S_a for the prototype is 6.64 m/s^2 and to get the same for the model following calculation is made.

Earthquake records have a time step of 0.01s and the calculation of the time step for the model is as given:

$$\Delta t_{model} = \frac{\Delta t_{prototype} \times T_{model}}{T_{prototype}} \qquad (23)$$

$$\Delta t_{model} = \frac{0.01 \times 0.019}{0.15} = 0.0013$$

Figure 3.9 and Figure 3.10 show the averaged ground input motions and the response spectra of seven records for the prototype, which have normal ones, and for the model, which have compressed ones. In Figure 3.9, threshold acceleration value (which is generally taken as 0.05g or 0.1g) above which earthquake ground motion is regarded as potential threat for structures has been demonstrated at the level of 0.1g.

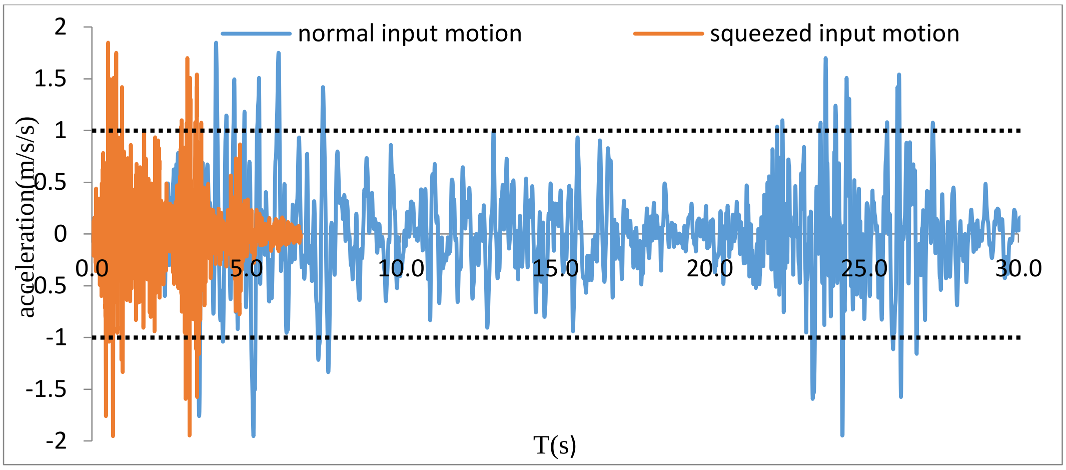

Figure 3.9 peak ground acceleration for the prototype and for the model

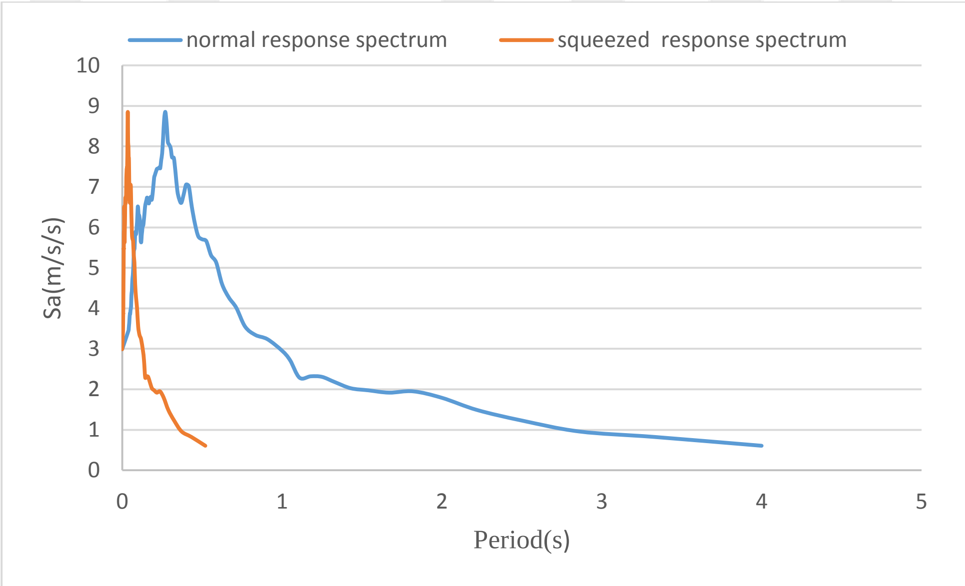

Figure 3.10 spectral accelerations of the prototype and the model

The other way to make sure that the model is behaved in a way in which it represents the prototype in all aspects by keeping the S_a the same is to increase the PGA of the ground motion for the model. It is worth noting that, while the PGA is increased, the period of the prototype and the model should be the same. However, in this project, this principle is not been implemented to the selected ground motion.

3.1.10 Modelling of the prototype and the model in GSA (one-storey/fixed base)

In GSA, firstly, fixed base one-story structure has been modelled and, subsequently, selected earthquake ground motion has been shifted, as expressed in the section 3.1.9, to make it suitable for the model. At the same time, the properties of the model has been assigned with reasonable values and modelled in GSA (Figure 3.11).

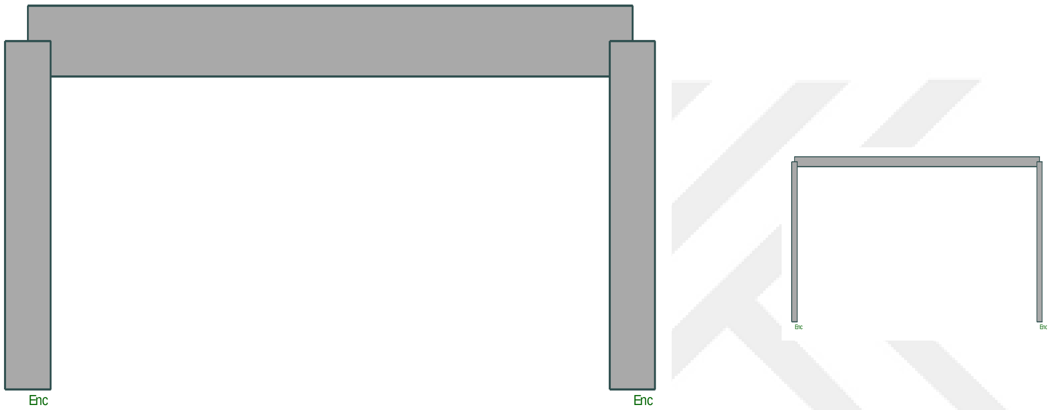

Figure 3.11 modelling of the prototype and the model in GSA, respectively

The reasons to model both the prototype and the model as a fixed base in GSA can be said that:

- It is, firstly, needed to assign the sizes of the model elements, rather than designing the model with rubber bearings and sizing them which makes the task difficult to challenge,
- ratio of the displacement of the fixed base prototype to that of the fixed base model can be used to obtain properties of the scaled bearing.

3.1.11 Modelling of the samples(the prototype and the model) with bearings

After obtaining the properties of the fixed base prototype and the model , they are decoupled by the bearings from the ground. While the properties of the bearing(HDRB) for the prototype has been given in the section of 3.1.2, it is crucial to procure the features of a bearing type material for the model.

The prototype has been modelled with HDRB (Figure 3.12), and the displacement has been obtained by applying earthquake force. The bearing is also modelled as one element to check the lateral displacement. By using the displacement ratio from fixed base models, the displacement expected from the scaled bearing has been found (the results are given in the result section).

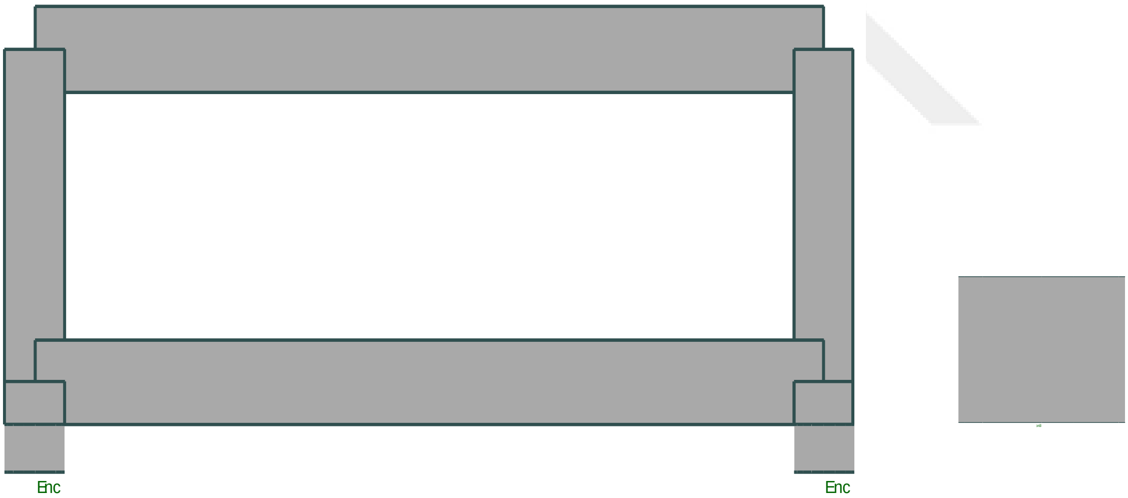

Figure 3.12 the modelling of the one-storey isolated real structure and the bearing only, respectively

The forces applied to the one-storey real structure or alternatively to the full rubber bearings and to the model are assigned as a quarter (1/4) of the forces applied to the fixed base prototype and fixed base model. The reason for that is because in the four-storey structure there are four HDRBs which are positioned to the corner of the structure. While the 3-D structure has been simplified to the 2-D, the features of the bearings were not changed at all. Because of that, the seismic forces are divided to 4, rather than 2 and noting that the earthquake forces for 3-D structure is assumed to be same with those of 2-D structure.

Stiffness calculation for the spring, where it is needed to design instead of scaled bearing, is done by means of below formula:

$$K_S = \frac{G_R}{t} \tag{24}$$

K_S is the stiffness of the spring
G_R is the shear modulus of the bearing
t is the thickness of the bearing (in this project, t is regarded as the height of the bearing)

Chapter 4

4.1 Results and Discussions

4.1.1 Results of four-story RC structure modelled in GSA

The four-story structure has been modelled two times in GSA, first one as fixed base and second one as base isolated. The results of story displacements are provided in Table 4.1 for fixed base and base isolated type structures and periods are 0.67 s and 0.68 s, respectively.

Table 4.1 displacement results

displacement(m)	fixed base	base isolated
first storey	0.012	0.012
second storey	0.025	0.024
third storey	0.043	0.041
fourth storey	0.057	0.054

As it is expressed in the study of Sato et al. (2011) that, the results for fixed base and base isolated structure are not so different from each other due to the fact that shear wall resists both gravitational loads and earthquake loads. Thus, it can be said that the contribution of the HDRB has not been observed explicitly because of dominant contribution of the shear wall in the response of the structure to the earthquake loads.

4.1.2 Results of fixed-base structures

As explained distinctively in the section 2.1.3 of this study, "the adequate model", which is based on "first-order similarity", has been used as a structural model.

To obtain reasonable representative model for the prototype, regarding the capacity of available shaking table, beam and column lengths are scaled by a factor of 1/10 (where the value of 1/10 is regarded as length scale factor), while the depths and widths of them are shortened by multiplications with the scale factor of 1/34. The material selected for the model is steel whose young's modulus is assumed as 2×10^8 (KN/m^2) and, thus, the scale factor for young modulus of material is 6.67.

In this study, it has been targeted to keep the sizes of the model elements, mass and the period of the model in the acceptable values (as can be seen in Table 4.2) so that:

- The model can represent the real structure reasonably well on the available shaking table
- The displacement of the model can be observed between the range of 0.1-130 mm, which are the minimum and maximum value that can be measured by available laser.

The load step for the model was obtained as 0.0013 in the section 3.1.9 of this study. Following that, time-acceleration and period-spectral acceleration (response spectra) graphs have been squeezed by scale factor of 0.13, keeping Sa the same. Substantially, depending on the period of the model (0.019 second), spectral acceleration has been selected and earthquake force has been computed.

REXEL directly gives average ground input motion of the records. When that motion has been introduced in GSA analysis, the results obtained have been identical to the average results of seven earthquake records (Table 4.2 and Table 4.3, respectively).

The table below demonstrates the mechanical and physical properties and earthquake results of one-storey prototype and one-storey model which are both **fixed based.** (The results are obtained depending on average motion of seven records.)

Table 4.2 properties of the prototype and the model

Property	Real(Prototype)	Relationship	Model	Scale factor*
E (KN/m^2)	30×10^6	E_P/E_M	200×10^6	6.67
Storey number	1	S_P/S_M	1	1
L_C (m)	4.95	L_P/L_M	0.495	1/10
L_B (m)	10	L_P/L_M	1	1/10
C_{BD} (m×m)	0.75×0.75	P^4/M^4	0.022×0.022	1/1.35E+06
B_{BD} (m×m)	0.3×1	P^4/M^4	0.009×0.03	1/1.24E+06
Mass (KN)	1900	M_P/M_M	0.25	1/7.6E +03
T (second)	0.15	T_P/T_M	0.019	1/7.9
$\ddot{u}_{gmax}$(m/s^2)	3	$PGA_{(P)}/PGA_{(M)}$	3	1
S_a (m/s^2)	6.64	$S_{a(P)}/S_{a(M)}$	6.64	1
P (KN)	1261.6	P_P/P_M	0.166	1/7.6E+03
$\delta(mm)$	15.5	δ_M/δ_P	0.378	1/41
Δt $(second)$	0.01	$\Delta t_{(P)}/ \Delta t_{(M)}$	0.0013	1/7.9

(*Scale factor are multiplied by prototype values to obtain model ones)

Table 4.3 results of each earthquake record and their averages

	PROTOTYPE			MODEL		
Eq. No	$S_a(m/s^2)$	F(KN)	δ(mm)	$S_a(m/s^2)$	F(KN)	δ(mm)
1	5.58	1060.2	13	5.58	0.14	0.316
2	6.84	1300	16	6.84	0.17	0.385
3	8.37	1590	19.5	8.37	0.21	0.475
4	8.52	1620	19.9	8.52	0.213	0.48
5	6.21	1180	14.5	6.21	0.155	0.35
6	5.03	955.7	11.7	5.03	0.126	0.285
7	6	1140	14	6	0.15	0.35
average	6.64	1263.5	15.5	6.64	0.166	0.378

It is worth noting that each earthquake and its PGA are scaled to target response spectrum and value of 3, respectively.

Based on Table 4.2, above interpretations can be made:

- 0.378 mm displacement in the model represents 15.5 mm displacement of the prototype.
- The mass ratio is equal to force ratio and, thus, it can be interpretted that earthquake force applied to the structure is directly proportionate to the mass.
- Furthermore, once the ground input motion has been compressed for the model by keeping spectral acceleration (S_a) constant, scale factor for time step, which is equal to 1/7.9, has became equal to that of period.

The obtained displacement for the model can be measured properly because obtained value (0.37 mm) is bigger than likely measurement accuracy of the model on the shaking table by using the laser which is 0.1 mm under the sine wave force. Moreover, 0.166 KN force applied to the model is smaller than the maximum force capacity of 20 KN.

4.1.3 Results of the one-storey prototype with rubber bearings design

Firstly, the rubber bearing has been designed as a single element (Figure 4.1). After that, a quarter of the earthquake force (1261.4/4=315.4KN) has been applied and 0.74 m displacement has been obtained.

To observe the behaviour of the rubber bearing in the structure, rubber bearings are designed, ignoring their periods, with one-storey real structure with suitable boundary conditions in GSA (Figure 4.2). For each rubber bearing, 315.4KN earthquake force has been applied to the structure and 0.74 m displacement has been attained, which is the same with that of single rubber bearing.

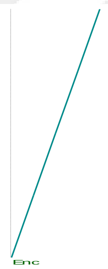

Figure 4.1 displaced shape of single rubber bearing (δ=0.74m)

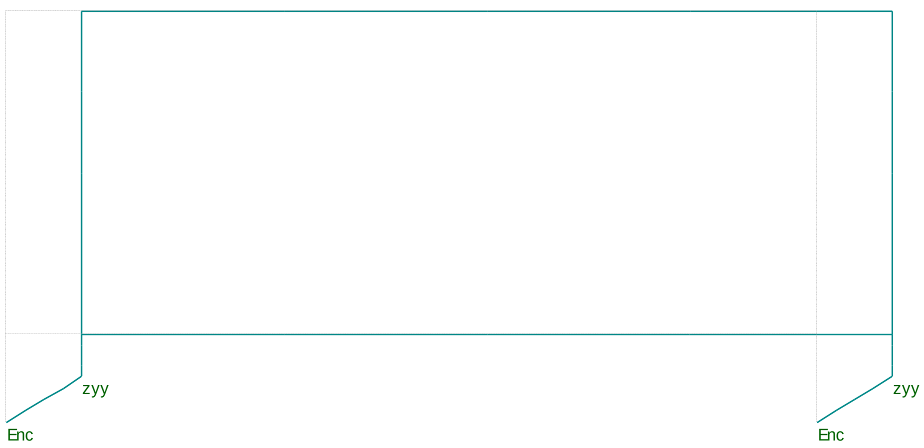

Figure 4.2 the shape of the structure under earthquake load of 630.8KN (δ=0.74m)

4.1.4 Results of the model with rubber type material

Once the displacement of the base isolated real structure or the full-scaled rubber bearing is calculated, the expected displacement from the model or scaled rubber bearing should be obtained.

Displacement ratio for the fixed base prototype and the model is (based on Table 4.2):

$$\frac{\text{real displacement}}{\text{model displacement}} = \frac{15.5\text{ mm}}{0.378\text{ mm}} \cong 41$$

This ratio should be the same with displacement ratio of the rubber bearings (full scale divided by scaled) or that of the base isolated prototype and the model. Thus,

$$\frac{\text{full rubber bearing displacement}}{\text{scaled rubber bearing displacement}} = 41 = \frac{0.74\text{ m}}{\delta_{\text{model with scaled bearing}}}$$

$\delta_M = 0.018\text{ m} = 18\text{ mm}$

Based on this result, it is needed to design the model with rubber bearings or that type of materials that can exhibit 18 mm displacement under earthquake force, which is in the measurable range of displacement.

Firstly, the rubber bearing (HDRB) has been used as a base isolation for the model and several of dimensions for the bearing has been acquired (the samples can be seen with their properties in Table 4.4). (The young's modulus and shear modulus of the rubber bearing are 1400 MPa and 0.62 MPa, respectively).

Table 4.4 different dimensional high damping rubber bearings and aspect ratios

Bear-ing no.	Height(H) (mm)	Width(W) (mm)	Depth(D) (mm)	Displa.(δ) (mm)	H/W	W/D	δ/W	A (mm^2)
1	20	10	9	18	2	1.1	1.8	90
2	40	20	9	18	2	2.2	0.9	180
3	18	10	8	18	1.8	0.8	1.8	80
4	14	8	8	18	1.75	1	2.25	64
5	32	12	12	18	2.67	1	1.5	144

In the practical uses of the HDRB, they can be shaped as circular or rectangular as examples given in the study of Marioni (1998) and their diameters and widths or depths are over two times bigger than the heights (in this project, the diameter of the real bearing is assumed to be 1.4 times bigger than its height). Moreover, width and depth values of a pad bearing are given as almost the same for real application. In the light of these explanations, based on Table 4.5, it can be said that the pad bearings seem to represent the real application in terms of width and depth ratios, except from sample 2. However, in respect to height to width ratios, all of them cannot seem to be reliable in real practice (for scaled base isolation experiment) because heights of the bearings are almost twice bigger than width and depth values which is the inverse of the real application.

In spite of H/W ratios of the samples, the samples can be acceptable depending on the displacement value which is 18 mm and its effect on the properties of the bearing. The reason for that is huge values for horizontal displacement have an impact on the effective shear modulus, the damping ratio, the height and overturning of the bearing(Nagarajaiah and Ferrell, 1999). Therefore, the stability issue should be carefully investigated for the experimental use of the samples. The critical load and horizontal stiffness of the samples at 18mm displacement should be computed and assessed in relation to stability interest. In this respect, it is also important to note that, it is experimentally proved by Buckle et al. (2002) that the bearing has a considerable strength capacity of critical load at the displacement that is equal to bearing width. Because of that, without considering critical load capacity it is hard to say that they are suitable or not with their sizes for scaled base isolation experiments.

It is also crucially essential to say that rocking motion effect which depends on the aspect ratios of the model are not taken into consideration when the sample sizes are assigned.

The shear modulus and the stiffness of above dimensioned bearings at 18 mm displacement are given in the below Table 4.5. The aim in the calculation of the stiffness is to use linear spring (rubber band) instead of bearing if the bearing is not applicable to the model in physical testing. The behaviours of the bearing and spring in the GSA model analysis at 18 mm displacement is exhibited in Figure 4.3 and Figure 4.4.

Table 4.5 shear modulus and stiffness of the high damping rubber bearings

Bearing no.	$\tau(\frac{N}{mm^2})$	γ **(Shear strain, %)**	$G(\frac{N}{mm^2})$	**K h(N/mm)**
1	0.46	90	0.51	2.3
2	0.23	45	0.51	2.3
3	0.52	100	0.52	2.3
4	0.65	130	0.5	2.3
5	0.3	56	0.54	2.3

When the lateral displacement has been taken place, shear modulus of the rubber bearing has dropped, as expected, to around 0.5 MPa from 0.62 MPa at 18 mm displacement. It can also be said that the shear strain values of the samples are appropriate because of the bearing ability to displace in large number with relation to its height. For instance, in the book of Virdi et al. (1997) it has been experienced that shear strain value of the rubber bearing, which has 600 mm diameter with 132 mm rubber thickness, can be from 0% to 250% in response to variety of lateral forces.

When the bearing is designed as a linear spring with 2.3 KN/m stiffness, the displacement is observed as the same with that of the model designed with rubber bearing.

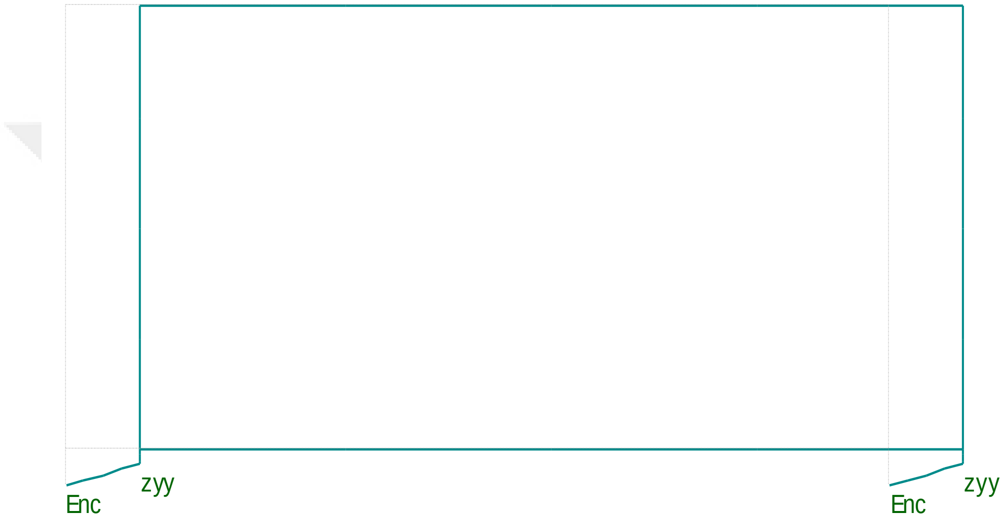

Figure 4.3 displacement of the isolated model with rubber bearing

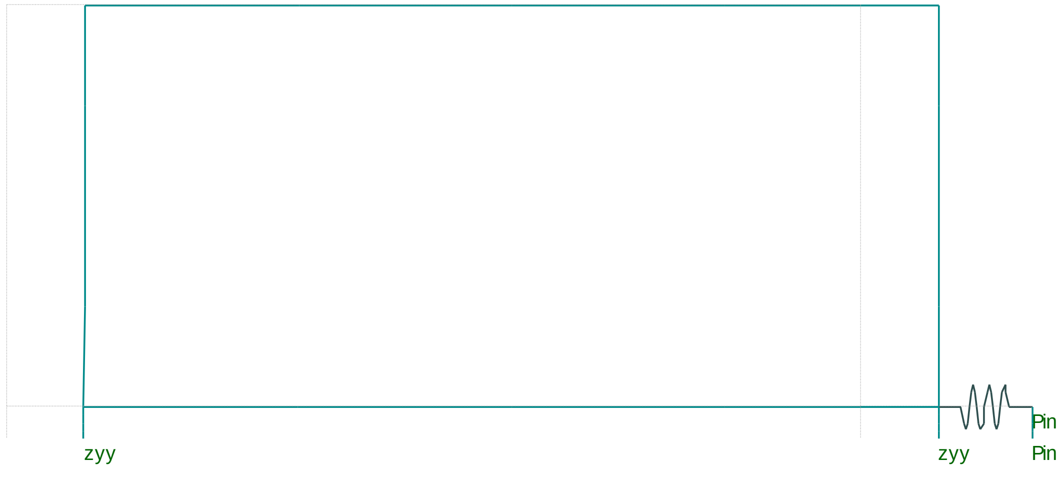

Figure 4.4 displacement of the isolated model with linear spring

Secondly, if only rubber material used instead of rubber bearing (which consists of rubber +steel), following dimensional bearings presented in Table 4.6 have been obtained (Rubber itself has a young modulus of 100MPa and a shear modulus of 0.3 MPa.).

Table 4.6 dimensions and aspect ratios of the sample bearings (only rubber included)

Bearing no.	Height(H) (mm)	Width(W) (mm)	Depth(D) (mm)	Displa.(δ) (mm)	H/W	W/D	δ/W	A (mm^2)
1	20	12	16	18	1.67	0.75	1.5	192
2	30	20	14	18	1.5	1.43	0.9	280
3	60	40	14	18	1.5	2.85	0.45	560
4	40	24	16	18	1.67	1.5	0.75	384
5	80	25	32	18	3.2	0.78	0.72	800
6	20	18	10	18	1.1	1.8	1	180

Based on results obtained by using rubber properties shown in Table 4.6, in respect to real applications of the pad bearing, for example the bearings studied by Nagarajaiah and Ferrell (1999), it can be said that the samples are not practical for scaled base isolation experiments because width and depth values are not close to each other. Furthermore, H/W ratios are not identical to the real practical values which are generally less than 1. Thus, it can be concluded that the samples do not represent the real bearing in those respects but, again, it is possible to have acceptable samples within them because it is all about stability issues, rocking motion effect and practicality.

Shear modulus and lateral stiffness of the samples have been given in below Table 4.7

Table 4.7 shear modulus and stiffness of the bearing (only rubber included)

Bearing no.	$\tau(\frac{N}{mm^2})$	γ (Shear strain %)	$G(\frac{N}{mm^2})$	K_h (N/mm)
1	0.216	0.9	0.24	2.3
2	0.148	0.6	0.246	2.3
3	0.074	0.3	0.246	2.3
4	0.108	0.45	0.24	2.3
5	0.052	0.225	0.23	2.3
6	0.23	0.9	0.25	2.3

From the above results, it is difficult to conclude that one of them has an advantage over another. However, once a number of different dimensional bearings has been obtained, the focus is going to be on the stability and the practicality of the bearing sizes.

While, in this project, there is not too much consideration and calculation about stability issues and rocking motion effect, it has been willing to select dimensions of the bearing with reasonable values. Moreover, the periods of the bearings (HDRB) have not been taken into account in the GSA analyses.

From the view of the stiffness, when the application of the bearing sizes is unlikely to be dimensioned for experimental study, then, the best idea for this issue in this project is to use linear spring (rubber band) which has a stiffness of the bearings. This methodology has been implemented in this project, as Figure 4.4 is provided for the spring modelling in GSA, and same displacement has been observed for each sample under the same lateral force.

Chapter 5

5.1 Conclusion

To assign the properties of the model, one story prototype and seven earthquake records have been utilized. It has been showed that the prototype can be represented by the model on the available shaking table as a fixed base with given properties and length scale factor of 1/10 shown in Table 4.2 by compressing ground input motion with scale factor of 0.13 while Sa is kept constant. It is also concluded that the results of average ground motion for the prototype and the model are equal to averaged results of each earthquake motion of seven records.

By using displacement ratio of the fixed base ones, the desired displacement from the scaled base isolation is computed as 18 mm, which is in the range of measureable values (between 0.1 mm and 130mm) by the available laser. The scaled bearings which have been featured as HDRB (steel + concrete) and rubber have been provided with different dimensional sample number of 5 and 6, respectively. It is observed that the shear modulus of them has decreased with roughly %16.2 (for HDRB) and %20 (for rubber) at 18mm displacement.

While the shear modulus and stiffness of each sample is around the same with another samples within the same type, it is hard to select one of them (HDRB or rubber) as a scaled base isolator. However, it can be interpreted that scaled HDRB can be beneficial to use due to the fact that, W/D ratio of the samples are close or equal to 1, as seen in real applications (discussed in result and discussion section with given relevant reference studies), which means they have square cross area, with the exception of sample 3 which has the ratio of 2.2.

Conversely, from the perspective of H/W ratios, the samples obtained by using rubber properties can be logical to select since their H/W values are smaller than that of HDRB. There are one exception in each type that cannot be included in latter case (according to H/W ratio):

(1) the sample 1 of HDRB has H/W ratio of 1 which is even smaller than all samples of that of rubber and (2) the sample 6 of the rubber has H/W ratio of 3.2 which is even bigger than that of all HDRB samples.

Finally, it can be concluded that even though the samples of both HDRB and rubber for the scaled base isolation do not resemble the real pad rubber bearing dimension ratios, there is a possibility that the samples can be valid. To prove that, however, it is greatly important to consider critical load and horizontal stiffness values at 18 mm displacement in relation to stability of the bearings. Moreover, rocking motion effect can also be regarded. If the samples are not practical, the best idea concluded in this project for experimental study is to use rubber bands which have total stiffness of the scaled bearings and use frictionless balls at the base of the model.

5.2 Future Work

Throughout the project study, all job is done in order to reach the aim which is "identification of materials suitable for scaled base isolation experiments and characterization of their properties". While the aim has been reached in an analytical way thanks to GSA computer software package program and properties of HDRB and rubber have been identified, for further study or more comprehensive study, natural periods of the bearings should be taken into account.

Although the dimensions of the scaled bearings (samples) for HDRB and rubber have been analytically assigned, to make sure that whether the desired behavior can be observed or not, shaking table test (physical testing) should be done to prove the results physically. It may raise that the layer numbers and thickness of the steel and rubber (scaled HDRB) may make them hard to do in practice because of small dimensions. It can also be questionable that the functions of the HDRB and rubber can or cannot be captured in such a small dimensional sample under the seismic action.

The obtained bearing samples may or may not be critical to stability in respect to critical load and rocking motion depending on axial load, shear modulus and stiffness, width of the bearing at a specific displacement. Therefore, it can be meaningful to regard the scaled bearings as to critical load and rocking motion effect.

For the shaking table test, if the samples are not practicable to test, it can be appreciable to use frictionless balls and rubber bands in further study. Once the model is attached to the frictionless balls on the shaking table and the rubber bands, whose total stiffness is equal to that of scaled rubber bearings, are tied with the model at floor level, the earthquake force can be applied. After that, the experimental results can be compared with the analytical results obtained in this project.

5.3 Summary

In the recent decades, the damage and human casualty of the seismic actions have been enormously diminished with the improving validity and design of the base isolation systems. Elastomeric bearing, lead rubber bearing and sliding bearing are well-known types of the base isolation system that they provide low input energy to the superstructure while they exhibit large lateral deformation under the seismic loads. Even though this benefit of base isolators has been appreciated, they may lead to increase in the inter-story drift because of the increase in the vertical acceleration.

To observe real behavior of the structure decoupled by a base isolation system from the foundation which is needed for design consideration, it is one of the best ways to do shaking table test. The important part of the shaking table testing is to scale the properties of the structure elements down by considering the capacity of available shaking table. A material that can be used in a model of the real structure and the real base isolation on the shaking table is a key issue to define since it is difficult to represent a superstructure with such a small scaled model.

Through this project, it is aimed to define materials and assign their properties for scaled base isolation testing. To do that, following steps have been followed;

1) The review of the isolation types, "structural model" and properties of some material has been done. After that, a real base isolated structure (four-story medical RC building), which has been studied before, has been selected for this study and has been simplified as 2-D structure. The isolation of the structure is HDRB in circular shape with 0.75 m diameter and 0.55 m height that has a shape factor of 36.75.

2) To select seven earthquake ground motions from European Strong-Motion Data, REXEL computer program has been utilized in relation to a location having latitude of 39,314° and longitude of 16.215° in Italy and each record has been scaled to target spectrum (where PGA is scaled to 3 m/s^2). The results of averaged motion of seven records and average results of them have been computed in the computer analyses (linear-elastic) and it is concluded that both ways give same results. Moreover, for computer modelling of the structure and its model, GSA computer software has been used and, as a first analysis, four-storey RC structure has been designed as fixed and isolated base. It is observed that the results of them are almost the same because of the shear wall.

3) Only first-story of the real structure (prototype) has been considered to apply scaling laws and similitude requirements. The periods of the prototype and its model (both are considered as fixed base) are 0.15 s and 0.019 s, respectively. To make earthquake ground motion suitable for the model, the time step has been changed to 0.0013 from 0.01 by keeping Sa the same, 6.64 m/s^2. The displacement of the prototype and the model is found as 15.5 mm and 0.378 mm in GSA analyses, successively.

4) The prototype, then, was modelled with HDRB and analysed while the period of the bearing is not taken into account. Depending on the obtained displacement from that analysis (which is 0.74 m), the expected displacement value from the scaled base isolation has been computed as 0.018 m by means of the displacement ratio between fixed base prototype and the fixed base model (which is equal to 41). Two materials, namely HDRB (steel + rubber) and rubber whose young's modulus and shear modulus are 1400 MPa, 100 MPa and 0.62 MPa, 0.3 MPa, respectively, are used for scaled base isolation. 5 different sized samples

for HDRB and 6 various dimensional samples for rubber have been attained with 0.018 mm displacement in GSA.

5) Each sample for scaled base isolation has been assessed in three ways: (1) height (H) to width (W) ratio, (2) width (W) to depth (D) ratio and (3) displacement (δ) to width (W) ratio. As observed in real applications of the pad bearings that, H/W ratio is generally between around 0.5 and 1, W/D ratio is around 1 and δ/W ratio is not desired to be over 1. From the perspective of H/W, no value of samples of both HDRB and rubber material is at that range but sample 6 of rubber material is most likely one to close to real value range with 1.1.

6) Samples of both types (HDRB and rubber) are close to full scale values in terms of W/D ratio, apart from sample 2 of HDRB and sample 2, 3, 6 of rubber. Lastly, δ/W ratio of sample 2 of HDRB and sample 2, 3, 4, 5 of rubber have values less than 1. Thus, it can be said that they may not be critical for critical load capacity.

7) Finally, it has been concluded that none of the samples of HDRB and rubber in scaled base isolation do not meet or liken the aspect ratios (H/W and W/D) and δ/W ratio of a real pad bearing, which have considerable effect on the overturning, rocking motion and critical load capacity of the bearing. Practicality or availability of the scaled bearings (samples) for shaking table test might also be a matter because of their sizes. Therefore, it might be a main step to consider stability and practicality of the samples for physical testing for further research on this study. It is also recommended that rubber bands can be alternative to the bearing application if the samples are not possible to apply in the shaking table test.

Reference List

Material selection and processing [Online]. CAMBRIDGE UNIVERSITY. Available: htpp://www-materials.eng.cam.ac.uk/mpsite/default.html.

AL-HUSSAINI, T. M., ZAYAS, V. A. & CONSTANTINOU, M. C. 1994. Seismic Isolation of Multi-story Frame Structures Using Spherical Sliding Isolation Systems. *NATIONAL CENTER FOR EARTHQUAKE ENGINEERING RESEARCH.* Buffalo: State University of New York.

AMBRASEYS, N., SMIT, P., SIGBJORNSSON, R., SUHADOLC, P. & MARGARIS, B. 2002. Internet-site for European Strong-Motion Data.

ANGLICANTAONGA 2011. Busted but not broken, says Fire Officer Bay.

ARYA, A. S. 1994. Concepts and techniques for seismic base isolation of structures. *Earthquake Engineering, tenth world conference.* Balkema, Rotterdam: University of Roorkee.

BRITISH STANDARD 2004a. Eurocode 2: Design of concrete structures. *General rules and rules for buildings.*

BRITISH STANDARD 2004b. Eurocode 8: Design of strucures for earthquake resistance. *General rules, seismic actions and rules for buildings.* BSI Standards Limited 2013.

BUCKLE, I., NAGARAJAIAH, S. & FERRELL, K. 2002. Stability of Elastomeric Isolation Bearings:Experimental Study. *JOURNAL OF STRUCTURAL ENGINEERING,* 128**,** 3-11.

CHUNG, W.-J., YUN, C.-B., KIM, N.-S. & SEO, J.-W. 1999. Shaking table and pseudodynamic tests for the evaluation of the seismic performance of base-isolated structures. *Engineering Structures,* 21**,** 365-379.

CONSTANTINOU, M. C., WHITTAKER, A. S., KALPAKIDIS, Y., FENZ, D. M. & WARN, G. P. 2007. *Performance of Seismic Isolation Hardware under Service and Seismic Loading,* Buffalo, The State University of New York.

DIHORU, L., CREWE, A. J., DIETZ, M. & TAYLOR, C. A. 2010. Physical Modelling and Specimen Testing. *Seismic engineering research infrastructures for european synergies.* Pavio: University of Bristol.

FENZ, D. M. & CONSTANTINOU, M. C. 2008. Spherical sliding isolation bearings with adaptive behaviour: Theory. *EARTHQUAKE ENGINEERING AND STRUCTURAL DYNAMICS,* 38**,** 163-183.

IERVOLINO, I., GALASSO, C. & COSENZA, E. 2010. Rexel: computer aided record selection for code-based seismic structural analysis. *bulletin of earthquake engineering,* 8**,** 339-392.

JEYASEHAR, C. A., KUMAR, K. S., MUTHUMANI, K. & LAKSHMANAN, N. 2009. Seismic performance evaluation methodologies for civil engineering structures. *Indian Journal of Engineering & Materials Sciences,* 16**,** 220-228.

JURCAU, C. S. & GILLICH, G.-R. 2009. The Use of Friction Pendulum Bearings for Isolation of the Built Environment 6**,** 87-90.

KALPAKIDIS, I. V. & CONSTANTINOU, M. C. 2009. Effects of Heating on the Behaviour of Lead-Rubber Bearings. I: Theory. *JOURNAL OF STRUCTURAL ENGINEERING,* 135**,** 1440-1449.

KELLY, J. M. 1997. *Earthquake-resistant design with rubber,* London, Springer.

KELLY, J. M. 1999. The role of damping in seismic isolation. *EARTHQUAKE ENGINEERING AND STRUCTURAL DYNAMICS,* 28**,** 3-20.

KELLY, J. M. & LAI, J.-W. 2011. The use of tests on high-shape-factor bearings to estimate the bulk modulus of natural rubber. *SEISMIC ISOLATION AND PROTECTION SYSTEMS,* 2.

KELLY, J. M. & MARSICO, M. R. 2013. Tension buckling in rubber bearings affected by cavitation. *Engineering Structures,* 56**,** 656-663.

LUCA, S.-G., CHIRA, F. & ROSCA, V.-O. 2005. Passive, active and semi-active control systems in civil engineering. *BULETINUL INSTITUTULUI POLITEHNIC DIN IASI,* 3**,** 23-31.

MALEKZADEH, M. & TAGHIKHANY, T. 2010. Adaptive Behaviour of Double Concave Friction Pendulum Bearing and its Advantages over Friction Pendulum Systems. *SCIENTIA IRANICA,* 17**,** 81-88.

MARIONI, A. 1998. THE USE OF HIGH DAMPING RUBBER BEARINGS FOR THE PROTECTION OF THE STRUCTURES FROM THE SEISMIC RISK *Jornadas Portuguesas de Engenharia de Estruturas*.

MOKHA, A. S., AMIN, N., CONSTANTINOU, M. C. & ZAYAS, V. 1996. Seismic Isolation Retrofit of Large Historic Building. *JOURNAL OF STRUCTURAL ENGINEERING,* 122**,** 298-308.

MOSTAGHEL, N. & KHODAVERDIAN, M. 1987. Dynamics of resilient-friction base isolator (R-FBI). *15***,** 379-390.

NAEIM, F. & KELLY, J. M. 1999. *Design of Seismic Isolated Structures From Theory to Practice,* Canada, John Wile & Sons.

NAGARAJAIAH, S. & FERRELL, K. 1999. STABILITY OF ELASTOMERIC SEISMIC ISOLATION BEARINGS. *JOURNAL OF STRUCTURAL ENGINEERING,* 125**,** 946-954.

OH, S.-H., SONG, S.-H., LEE, S.-H. & KIM, H.-J. 2013. Experimental study of seismic performance of base-isolated frames with U-shaped hysteretic energy-dissipating devices. *Engineering Structures,* 56**,** 2014-2027.

PATIL, S. J. & REDDY, G. R. 2012. State Of Art Review - Base Isolation Systems For

Structures. *International Journal of Emerging Technology and Advanced Engineering,* 2**,** 438-453.

RAO, P. B. & JANGID, R. S. 2001. Performance of sliding systems under near-fault motions. *Nuclear Engineering and Design,* 203**,** 259-272.

ROBINSON, W. H. 1982. Lead-Rubber Hysteretic Bearings Suitable for Protecting Structures during Earthquakes. *EARTHQUAKE ENGINEERING AND STRUCTURAL DYNAMICS,* 10**,** 593-604.

ROBINSON, W. H. & TUCKER, A. G. 1977. A Lead-Rubber Shear Damper. *BULLETIN OF THE NEW ZEALAND NATIONAL SOCIETY FOR EARTHQUAKE ENGINEERING,* 10.

ROUSSIS, P. C. & CONSTANTINOU, M. C. 2006. Uplift-restraining Friction Pendulum seismic isolation system. *EARTHQUAKE ENGINEERING AND STRUCTURAL DYNAMICS,* 35**,** 577-593.

SABNIS, G. M., HARRIS, H. G., WHITE, R. N. & MIRZA, M. S. 1983. *Structural modelling and experimental techniques,* the United State of America, Prentice-Hall.

SATO, E., FURUKAWA, S., JAKEHI, A. & NAKASHIMA, M. 2011. Full-scale shaking table test for examination of safety and functionality of base-isolated medical facilities. *EARTHQUAKE ENGINEERING AND STRUCTURAL DYNAMICS,* 40**,** 1435-1453.

SINDEL, Z., AKBAS, R. & TEZCAN, S. S. 1996. Drift control and damage in tall buildings *Engineering Structures,* 18**,** 957-966.

TOUAILLON, J. 1870. *Improvement in Buildings*. USA patent application.

TYLER, R. G. 1991. Rubber Bearings in Base-isolated Structures. *BULLETIN OF THE NEW ZEALAND NATIONAL SOCIETY FOR EARTHQUAKE ENGINEERING,* 24**,** 251-275.

VIRDI, K. S., GARAS, F. K., CLARKE, J. L. & ARMER, G. S. T. (eds.) 1997. *Structural Assessment:The Role of Large and Full-scale Testing.*

London: E & FN Spon.

WARN, G. P. & RYAN, K. L. 2012. A Review of Seismic Isolation for Buildings: Historical Development and Research Needs. *Buuildings,* 2**,** 300-325.

WILKINSON, S. M. & SIVASELVAN, M. V. 2008. Sensitivity of nonlinear frames to modelling parameters and earthquake excitations. *The 14th World Conference on Earthquake Engineering.* Beijing.

YOO, B. & KIM, Y.-H. 2002. Study on effects of damping in laminated rubber bearings on seismic responses for a 1/8 scale isolated test structure. *EARTHQUAKE ENGINEERING AND STRUCTURAL DYNAMICS,* 31**,** 1777-1792.